1975

A new adaptive delta modulation system

Hyun-Jik Kim
Iowa State University

INFORMATION TO USERS

This material was produced from a microfilm copy of the original document. While the most advanced technological means to photograph and reproduce this document have been used, the quality is heavily dependent upon the quality of the original submitted.

The following explanation of techniques is provided to help you understand markings or patterns which may appear on this reproduction.

1. The sign or "target" for pages apparently lacking from the document photographed is "Missing Page(s)". If it was possible to obtain the missing page(s) or section, they are spliced into the film along with adjacent pages. This may have necessitated cutting thru an image and duplicating adjacent pages to insure you complete continuity.

2. When an image on the film is obliterated with a large round black mark, it is an indication that the photographer suspected that the copy may have moved during exposure and thus cause a blurred image. You will find a good image of the page in the adjacent frame.

3. When a map, drawing or chart, etc., was part of the material being photographed the photographer followed a definite method in "sectioning" the material. It is customary to begin photoing at the upper left hand corner of a large sheet and to continue photoing from left to right in equal sections with a small overlap. If necessary, sectioning is continued again — beginning below the first row and continuing on until complete.

4. The majority of users indicate that the textual content is of greatest value, however, a somewhat higher quality reproduction could be made from "photographs" if essential to the understanding of the dissertation. Silver prints of "photographs" may be ordered at additional charge by writing the Order Department, giving the catalog number, title, author and specific pages you wish reproduced.

5. PLEASE NOTE: Some pages may have indistinct print. Filmed as received.

Xerox University Microfilms
300 North Zeeb Road
Ann Arbor, Michigan 48106

A new adaptive delta modulation system

by

Hyun-Jik Kim

A Dissertation Submitted to the
Graduate Faculty in Partial Fulfillment of
The Requirements for the Degree of
DOCTOR OF PHILOSOPHY

Major: Electrical Engineering

Approved:

Signature was redacted for privacy.

In Charge of Major Work

Signature was redacted for privacy.

For the Major Department

Signature was redacted for privacy.

For the Graduate College

Iowa State University
Ames, Iowa

1975

TABLE OF CONTENTS

1. BACKGROUND AND LITERATURE REVIEW

In communication systems the digitization techniques of the analog signals, mainly voice signals, are catching up and even threatening to surpass their counterparts in analog transmission, although it has been only two decades since the development of the first commercial digital transmission method called pulse code modulation. This trend toward digital communication systems is being accelerated by the advent of digital computers and simple integrated circuit (IC) building blocks. It is very likely that the tendency will go on since digitization techniques offer some advantages over analog techniques.

The advantages of digitization are summarized as follows [1]:

1. Unlike frequency-division multiplexing, no complex filters are necessary in time division multiplexing since the multiplexing functions can be accomplished with digital circuitry which is available at relatively low cost.
2. Switching of digital information can be easily realized with digital building blocks such as digital computers.
3. Secrecy and privacy are easily preserved, because the sequences of 1's and 0's can be scrambled easily.

4. Bennett and Davey pointed out that better noise immunity is possible in the transmission medium when the performance of straight analog vs. regenerative digital links is compared as a function of the number of links. For the analog case we can assume that the average noise power increases directly with the number of links and that the analog repeater maintains the same signal power at the output of each link. In the regenerative case it is assumed that each repeater has a very small independent probability of error. Then the probability of error in the digital channel with a regenerative repeater is much smaller than that of the analog channel for binary transmission with additive white Gaussian noises and with the same number of links [2].

5. Another advantage is also noted by Bargellini [3]. The frequency-division multiplexing (FDM) system employed by INTELSAT IV of COMSAT Laboratory is not as efficient as a time-division multiplexing (TDM) system with phase-shift keying (PSK) in digital transmission because of reduced efficiency in the travelling wave tube amplifier in the satellite. In other words, the weight and power requirements imposed on the spacecraft are greater for FDM. In

comparing the INTELSAT IV and a 1980 communication satellite using digital transmission one can predict that the number of usable channels per unit satellite weight for TDM is several times greater for FDM.

The main problem in digitization techniques is how to transmit the signals efficiently in digital form. There are other techniques for speech transmission such as those based on pitch excitations, vocal tract resonances, etc. [4, 5]. However, here we are mainly interested in straight reconstruction of the acoustic time waveform because of the resulting coder simplicity of implementation. In efficient digital coding, one might try to take advantage of variable length coding schemes such as the Huffman optimum coding scheme depending on the probability distribution function of the sequences after digitization of the signals [6, 7]. But the nonuniformity of the word length at each sampling instant, which in consequence requires buffer memories to transmit the bits synchronously, and the vulnerability of a catastrophic string of bit errors that may be caused by a transmission error made the variable length coding scheme unpopular.

Therefore, we here concentrate on achieving efficient digitization of time waveforms by using prediction methods based on information on the past amplitudes. Techniques

which have been proposed and investigated for the purpose are delta modulation (DM), well-known pulse code modulation (PCM), differential pulse code modulation (DPCM), adaptive differential pulse code modulation (ADPCM), and adaptive delta modulation (ADM).

In the research presented here, only adaptive delta modulations were investigated because of their relative simplicity and their promising characteristics. The aim of this research is to propose a new hybrid adaptive delta modulator and to compare it with other published adaptive delta modulators using the signal-to noise ratio as the performance criterion.

The characteristics of well-known systems will be explained briefly as follows:

1.1. Pulse Code Modulation (Figure 1.1) [8, 9]

Pulse code modulation, the first digitization technique, was invented by A. H. Reeves and is currently being widely used.

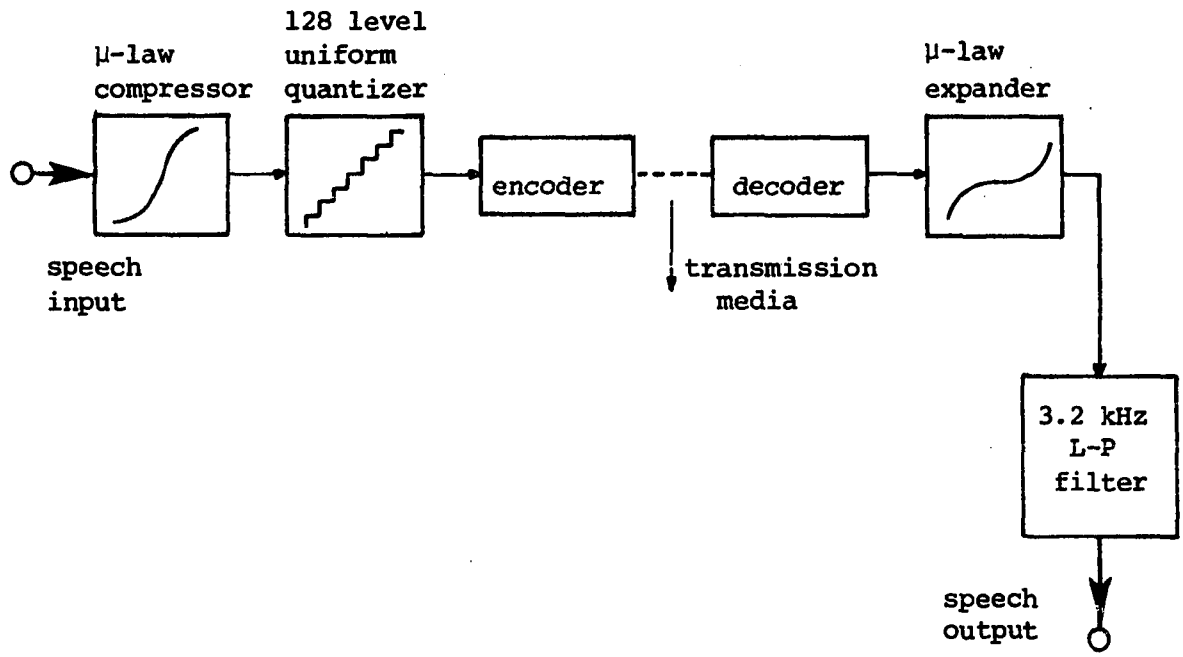

Figure 1.1. PCM system

It consists of a sampler (usually 8 kHz/sec) and a 128 level quantizer with 7 bits. To encode the signal effectively, a compressor at the transmitting end and an expander at the receiving end are added, since the signals of low amplitude are more probable than those of high amplitude. In other words, low amplitude regions of high probability are finely quantized and high amplitude, low probability regions are coarsely quantized.

The compression characteristics needed to give the least mean square error have been published for several probability distributions of the input signals, and several

optimum quantizers are published [10, 11, 12]. More details on determining the quantizers will be discussed in Appendix A.

The combination of a compressor and a uniform quantizer is equivalent to a nonuniform quantizer. One compression curve due to Smith [11] is given by

$$Y = \log (1+\mu x)/\log(1+\mu)$$

A value of μ on the order of 100 is considered acceptable in practical situations and $\mu = 255$ is currently used in actual implementation, mainly in North America.

The so-called A-law is also given by [8]

$$Y = Ax/(1+\log A) \qquad 0 \leq X \leq 1/A$$

$$= (1+\log Ax)/(1+\log A) \qquad 1/A \leq x \leq 1$$

A = 87.6 is widely used for speech companding on telephone circuits, particularly in Europe. The S/N ratio curve with A-law companding for 800 Hz sinusoidal waveforms sampled at 56 kHz is shown in Figure 4.1 (curve labeled number 3).

It is also possible to compress the signal digitally using code translation. Digital linearizable companding is attractive because it allows digital signal processing without necessity of decoding first to analog form, and finally encoding into digital form again.

The disadvantages of PCM system are the complexity of

the system and the relatively high bit rates.

1.2. Differential Pulse Code Modulation (Figure 1.2) [13, 14]

This sytem is an outgrowth from PCM system and is suggested to overcome high bit rates of PCM system and to encode signals more efficiently using slow variation of the amplitude of signals.

In DPCM system, the difference between the input signal and the output of a predictor which consists of delays in a feedback loop is coded by the nonuniform quantizer. At 8 kHz sampling rate it is well known that the correlation coefficients for speech signals are .8 for the band-pass filtered signals between 200 Hz and 3,200 Hz, and .85 for the 3,200 Hz low-pass filtered signals.

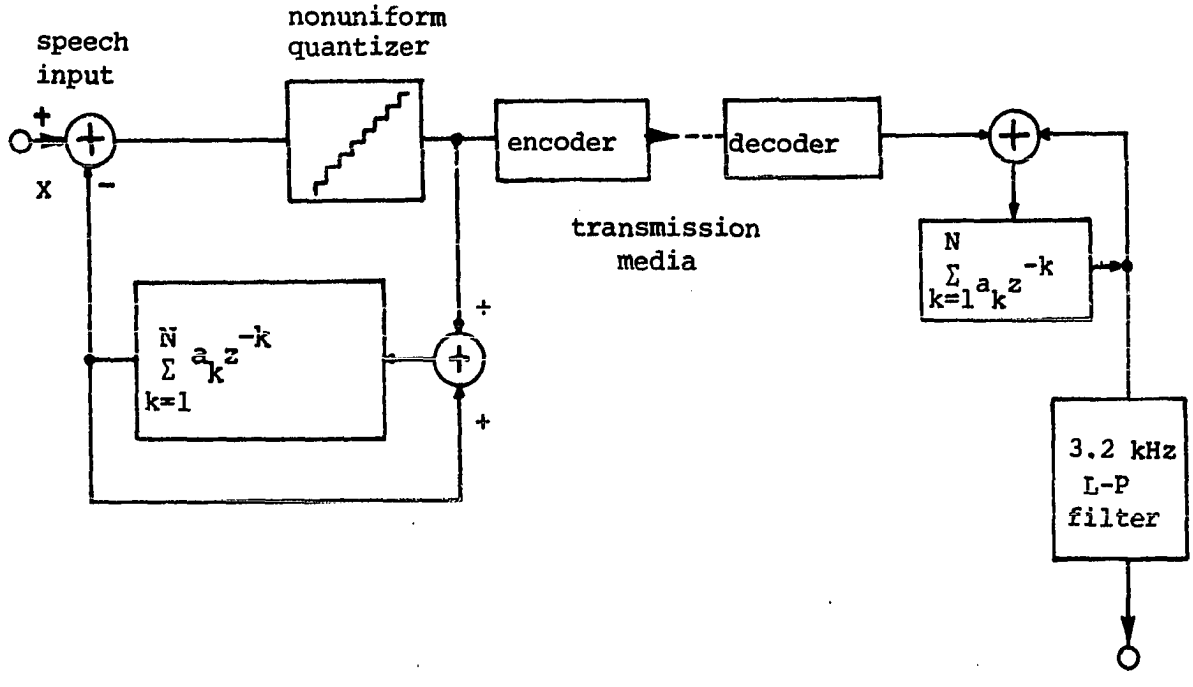

Figure 1.2. DPCM system

The mathematical verification of the advantage is as follows: Let us consider the variance of the two signals. We want to prove that the variance of the first difference

$$e_r = x_r - x_{r-1}$$

is smaller than the variance of x_r.

The variance and the expectation of the difference are given as

$$E(e_r) = E(X_r - X_{r-1})$$

$$\begin{aligned} Var(e_r) &= E\{e_r - E(e_r)\}^2 \\ &= E[X_r - X_{r-1} - E(X_r - X_{r-1})]^2 \\ &= E[X_r - E(X_r) - X_{r-1} + E(X_{r-1})]^2 \\ &= E[X_r - E(X_r)]^2 + E[X_{r-1} - E(X_{r-1})]^2 \\ &\quad -2E\{[X_r - E(X_r)][X_{r-1} - E(X_{r-1}]\} \\ &= Var(X_r) + Var(x_{r-1}) - 2\rho\, Var(X_r) \\ &= 2(1-\rho)\, Var(X_r) \end{aligned}$$

where

ρ is a correlation coefficient.

Since ρ is always greater than .5, $Var(e_r)$ is smaller than $Var(X_r)$.

A signal to noise improvement of 3 to 7 dB over PCM system or a saving of one bit per word is thus achieved [15] .

The benefits obtained from non-uniform quantizers in DPCM system are the same as those obtained from compression and expansion in the PCM system, because the probability distribution of the first differences of the signals has some resemblance to the original signals [16]. Some signal to noise ratio improvement in DPCM over PCM with the same non-uniform optimum quantizers is shown in Paez and Glisson [12].

Attempts have been made to find the coefficients, a_i's, in the predictor of DPCM system which minimize the variance of e_r [16, 17, 14]. For a one tap predictor where $a_i = 0$, $i = 2,3,...$ the predictor can be replaced by an integrator. The substitution is verified by the following identities.

The Z-transformation of the feedback portion (Figure 1.3) in DPCM is given by

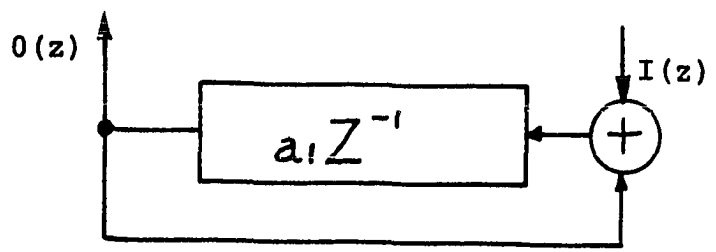

Figure 1.3. Feedback portion of a simple DPCM system

$$[O(z)+I(z)]\ a_1 z^{-1} = O(z)$$

Then, the transfer function is

$$T(z) = \frac{O(z)}{I(z)} = \frac{a_1 z^{-1}}{1-a_1 z^{-1}} = \frac{a_1 z}{z-a_1}\ z^{-1}$$

Using the identities [18]

$$\mathbf{Z}^{-1}\{z^{-m}F(z)\} = f(k-m)$$

where

$$\mathbf{Z}^{-1}[F(z)] = f(k)$$

$$\mathbf{Z}^{-1}\{\frac{z}{z-1}\} = 1$$

$$\mathbf{L}\{1\} = \frac{1}{s}$$

the corresponding Laplace transform of the transfer function T(z) is

$$\mathbf{L}\{\mathbf{Z}^{-1}[T(z)]\} = e^{-sT}\ \frac{1}{s}$$

where

$$a_1 = 1.$$

Since T is very small e^{-sT} approaches unity. The proof indicates that for a simple DPCM an integrator may replace the predictor.

1.3. Adaptive Differential Pulse Code Modulation (Figure 1.4)

ADPCM [16, 19, 20] has been recently developed to improve DPCM system by adapting the quantizer's step sizes in DPCM. Another approach is to adapt the coefficients a_i of the feedback loop of DPCM system. But it requires search techniques for minimum variances which are impractical due to computation complexity in most cases [16]. Stroh describes a straightforward estimation procedure for Gaussian signals [19]. The technique of Cummiskey, Jayant, and Flanagan [20] makes a more explicit use of 'overload' and 'underload' cues to provide an adaptation logic. They multiply 3 or 4 predetermined quantizer multiplication factors to the previous uniform quantizer interval sizes according to appropriate sequences. Their technique shows better signal to noise ratio (S/N) at the cost of a higher complexity of the system than other systems.

Recently Gibson, Jones and Melsa [21] uses the estimation theory of the Kalman filter with significant results, but the computation procedures are much too involved to be done in real time with currently available digital integrated circuit technology.

A reduction in bit rate was achieved by an adaptive dual-mode coding system which employs delta modulation for

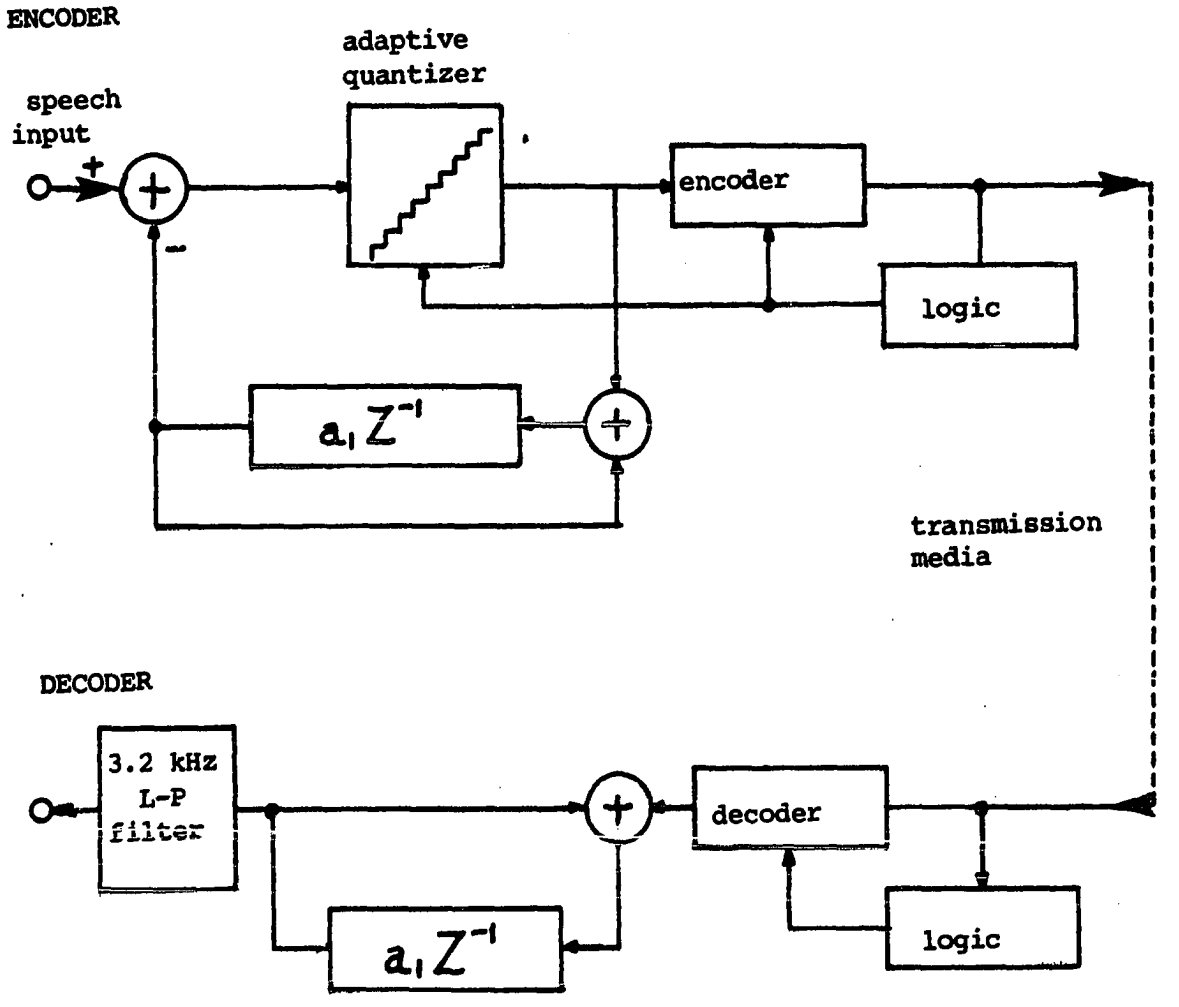

Figure 1.4. ADPCM system

signals with slow variation, and which employs differential pulse code modulation for signals with fast variation [22].

2. DELTA MODULATION

2.1. Linear Delta Modulation

A linear delta modulator (Figure 2.1) was first studied extensively by F. DeJager [23] in 1952 and has the advantage of extreme simplicity. It is the simplest DPCM with a two level quantizer. In delta encoding, the difference between the input signal and output of a predictor is grossly over-sampled above the Nyquist frequency, i.e. twice the highest input frequency. So the correlation coefficient is much

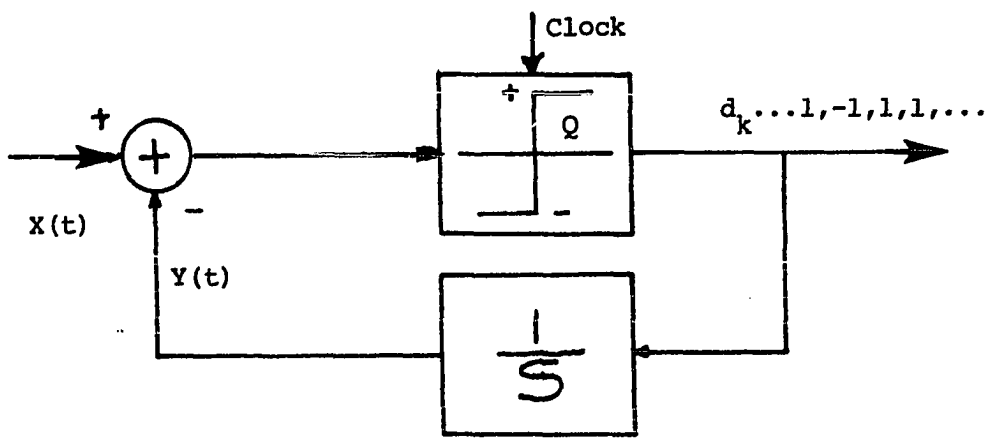

Figure 2.1. A linear delta modulator

closer to unity than that of PCM system with a sampling frequency of 8 kHz. The following equations describe a basic delta modulator:

$$Y(t_k) = d_k Q + Y(t_{k-1})$$

where

$$d_k = \text{sgn}\{X(t_k) - Y(t_{k-1})\}$$

Q = step size

with

$X(t)$ = signals to be coded

$Y(t)$ = predicted signals

For convenience of notation, 0 will be used instead of -1.

The integrator is a predictor which predicts that the input signal will not change from sample to sample. Sometimes double integration is employed above 1 kHz to about one-sixth of the sampling frequency with slightly better performance [1, 23]. Cummiskey claims no appreciable effect on S/N ratio using double integration [16]. The idea of double integration is merely to provide better signal prediction. The stability problem with double integration was investigated by Nielsen [24].

The constant step size in a linear delta modulator limits the performance to slowly varying signals. DeJager [23] showed that to achieve a compatible performance with a 7 bit log PCM system the sampling rate, i.e. bit rate, of a linear delta modulator must be approximately twice that of PCM. Two types of noises are defined in a delta modulator.

Here the noise is defined as the quantizing noise which is the difference between the input signal and the reproduced signal. However, the majority of noise power lies outside the telephone bandpass filter and the noise power is greatly reduced.

A. One type of noise is the slope overload noise (Figure 2.2). The slope overload noise is introduced by the small value of step size; i.e., the step size is too small to follow a steep segment of the input waveforms.

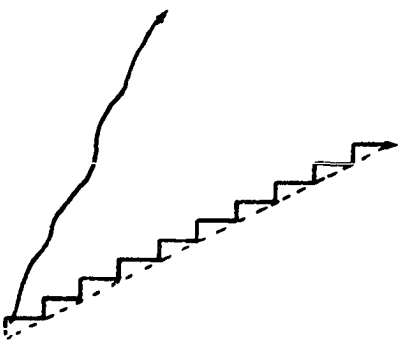

Figure 2.2. Slope overload noise

B. Another type of noise is the granular noise (Figure 2.3). The granular noise on the other hand is introduced by the large value of the step size; i.e., the step size is too large relative to the local slope characteristics of the input. For the given slope, it is therefore clear the relative small values of step sizes accentuate slope overload, while relatively large values of step sizes increase

granularity. It should therefore be possible to find the optimum step sizes to provide a minimum total error power

Figure 2.3. Granular noise

[25]. Even when the step size is optimized the performance of the modulator will be satisfactory only at a sampling frequency that may be undesirably high. As a consequence, the dynamic range is very narrow as proved theoretically and experimentally [26, 27].

There are several mathematically oriented papers on S/N ratio computation in a linear delta modulator. Due to different assumptions, the results vary from one to the other. Van deWeg [28], Goodman [29], Abate [25], and Schilling [30] (with a similar result to Goodman's) dealt with the granular noise. Protonotarios [31] (improving a formula derived by Greenstein [32] and Schilling and Taub [30] dealt with the slope overload noise. DeJager [2] derived the maximum attainable S/N ratio with sinusoidal inputs. O'Neal [26] published a paper on S/N ratio with Gaussian and television input signals. He assumed that the

quantizing noise consisted of two components, granular noise and slope overload noise, and that the total quantizing noise is simply their sum. Slepian [33] rigorously derived a procedure for computing the quantizing noise precisely without separating the noise into two components. O'Neal also investigated a possibility of using a linear delta modulator for transmitting data signals [34]. A typical S/N curve of 800 Hz sinusoidal input signals sampled at 56 kHz is given in Figure 2.4 [27]. The slope for low input power is due to granular noise produced by the rather large step sizes. The downward slope for high input signal power is accounted for by the inability of the predictor to follow the input, which means a slope overload noise.

2.2. Adaptive Delta Modulation

Adaptive delta modulators (ADM) [35, 36, 37, 38, 39, 40] have been proposed to improve the performance of a linear delta modulator while maintaining the simplicity of a linear delta modulator. The main advantage of an adaptive delta modulator is in changing the step size to cope with the changing input signals. By adapting the step sizes according to a nonlinear prediction of the changing input slopes, the adaptive delta modulators can squelch idle channel noise and extend dynamic range. The function of step size adaptation

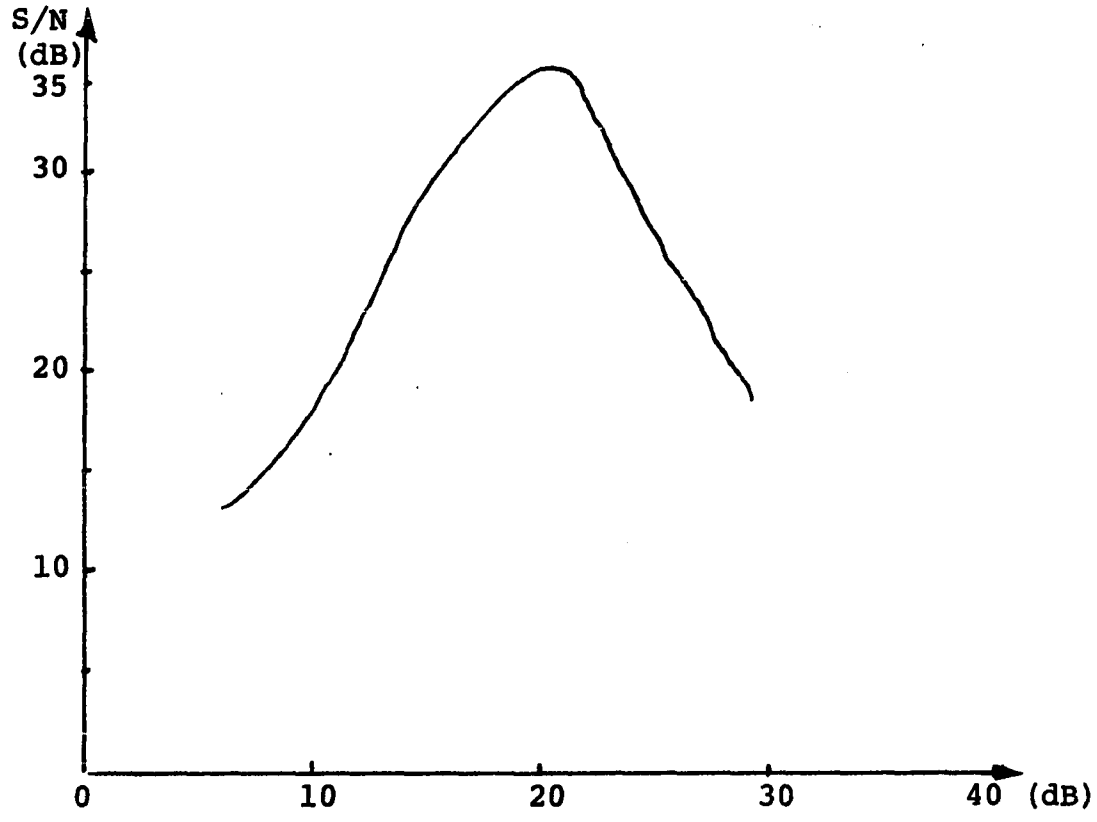

Figure 2.4. S/N curve of a LDM for the sinusoidal input

is to improve dynamic range and insure that the adaptive delta modulators are operating at or near their optimum step size for a wide range of signal power levels. It was shown [25, 27] that step size adaptation does not increase the maximum S/N ratio for adaptive delta modulators.

ADMs can be divided into two categories, analog and discrete, depending on the method used to retrieve information from the digital output which is then used to adjust the step sizes of the modulators.

A. Analog ADM: Most analog ADMs basically use a low-pass filter (100-200 Hz) and a rectifier to obtain low frequency energy from digital output sequences. The low frequency energy is used as the step size adaptation signal. If at a given time the quantization step is too small, i.e. slope overload is occurring, a series of consecutive ones and zeros (11111... or 00000...) will be generated at the output of an encoder. Hence, the bit stream acquires more low frequency energy which passes through the low-pass filter, causing the step size to grow larger. If the step size is too large the output oscillates between zero and one (101010...) most of the time, causing energy in the bit stream to shift out of the passband of the low-pass filter. This causes a drop in the adaptation voltage and a subsequent decrease in the quantizing step. By the nature of its adaptiveness, the analog ADM is suitable for rather slowly varying signals and is sometimes called a syllabic companding technique.

The following schemes have been proposed:

1. A. Tomozawa and H. Kaneko's companded delta modulation system (Figure 2.5) [37].

In this system the delta modulation encoder is a type of a feedback encoder and employs a syllabic companding technique. Companding is performed entirely in the local decoder in the transmitter and receiver.

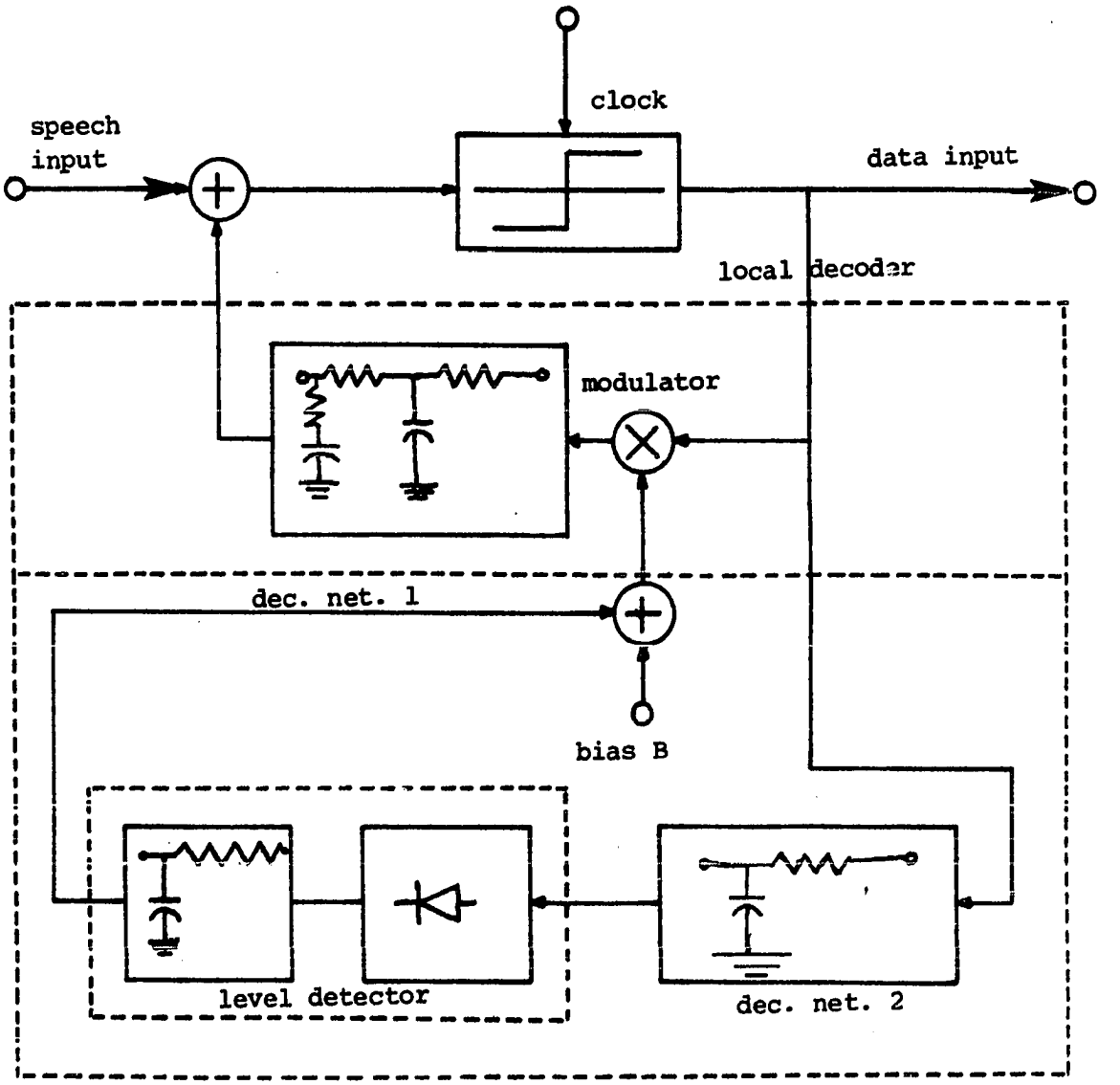

Figure 2.5. Tomozawa and Kaneko's companded ADM system

In the local decoder, coded pulses are fed into two decoding networks. The output of the decoding network 2 represents the modulating signal component contained in the coded pulses. A level detector develops a slowly varying d-c voltage according to the output level of decoding network 2, and the sum of this d-c voltage and the bias voltage B controls the amplitude of the coded pulses. These amplitude-modulated code pulses are fed to decoding network 1. The quantizing step size, which is proportional to the pulse height applied to decoding network 1, varies in accordance with the signal component in the coded pulses. The output signal level of decoding network 1 is proportional to the square of the signal component of the coded pulses. Therefore, the local encoder has a square-type expanding characteristic. At the receiver side, the same decoding circuit that was in the local decoder can be used.

2. J. A. Greefkes and F. DeJager's continuous delta modulation system [35].

The block diagram is shown in Figure 2.6.

The basic concept uses the frequency band below 100 Hz to transmit the information describing quantization step size. In order to accommodate two channels, slope detector and audio input, the speech signals must be limited to the 300 Hz to 3200 Hz band. After the incoming audio signal

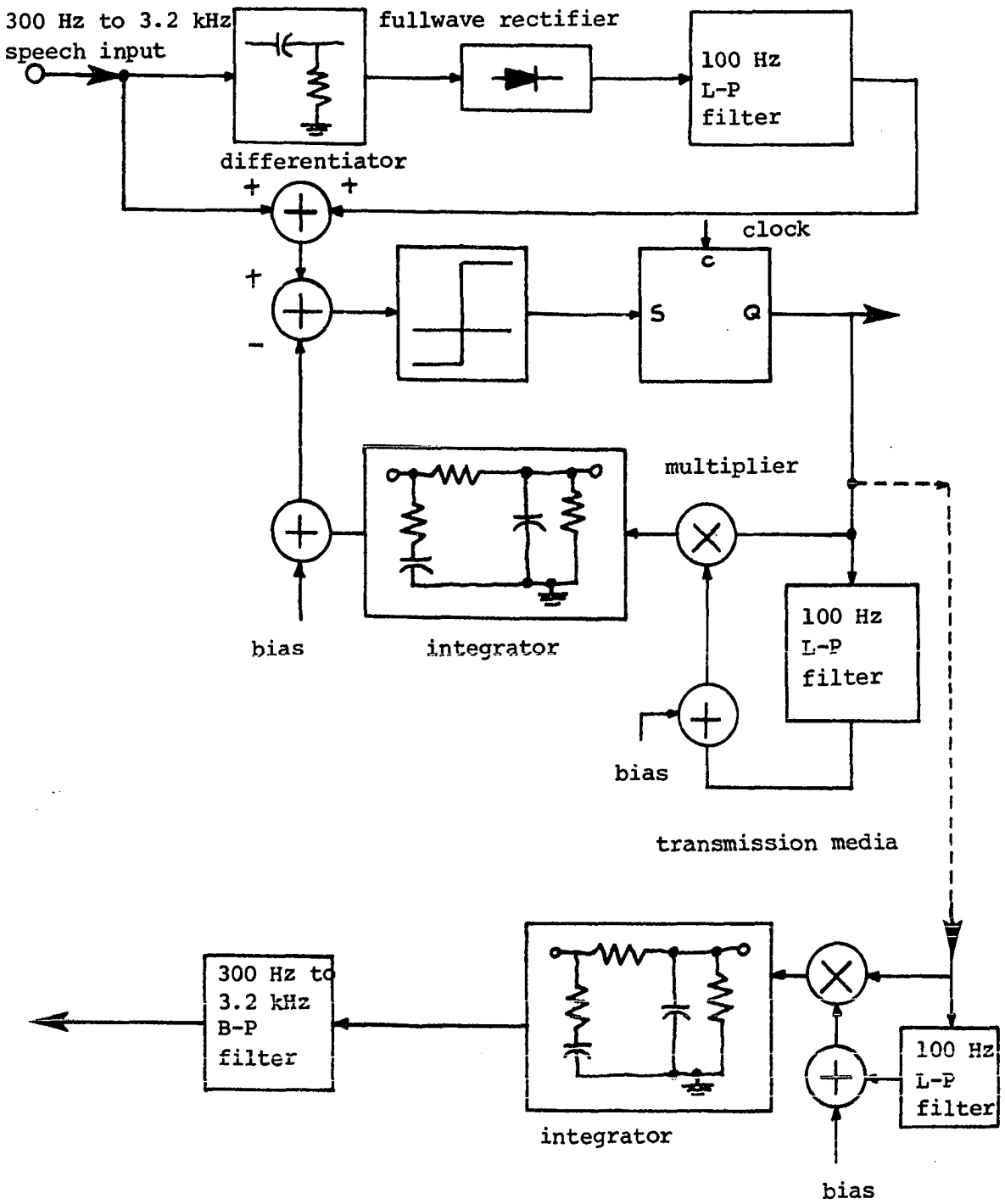

Figure 2.6. Greefkes and DeJager's continuous ADM system

is sent through a high-pass filter and split into two, one part is put through a branch consisting of a differentiator, a full-wave rectifier, and a smoothing filter. In this branch, the slope of the signal is determined and a measure of closeness to the overload level is obtained. The slowly varying signal is combined in a difference network (subtractor) with the high-pass filtered audio signal. The feedback path from the coder also leads into the same network. The coder is therefore fed by a combined input of three signals, one of which is a slowly varying d-c component. The bias in the feedback path controls the threshold level of the comparator.

3. Other systems: Excellent explanations and reviews for other similar systems are found in the literature [1, 41].

B. Discrete ADM: Discrete systems adjust step sizes by directly decoding the digital output sequences of the systems according to predetermined algorithms.

The idea of detecting consectuive 1's or 0's (11... or 000...) which correspond to slope overload distortion and alternating 1's and 0's (1010...) which correspond to granular noise originated from a linear delta modulation and is basic to understanding discrete ADM systems.

1. High Information Delta Modulation (HIDM): [40] The HIDM was the first ADM system to be proposed. The step sizes increase and decrease exponentially with time. In other words, the increment in step size is doubled, like 1,2,4,8,,,. when the polarity of the last two bits is the same. Then if the increment is too large, i.e. the polarity is not the same, the pulse direction reverses and the increment in step size is halved.

2. Jayant's ADM system: [39] N. S. Jayant explored the bit sequences more with computer simulations, which later was implemented by Cummiskey [41, 25]. This system is similar to other systems in the sense that it also mainly depends upon the last bit of the output.

The system is illustrated in Figure 2.7.

His system adapts its step size on the basis of a comparison between the last two bits. The previous step size is multiplied by $P>1$ or $Q<1$ depending on whether the polarity of the last two bits are the same or not, while maintaining $P \times Q = 1$. The condition $P \times Q = 1$ is a sufficient and necessary condition for stability in a long run. He found by simulation that $P = 1.5$ gives optimal results (maximum S/N ratio) for a band-pass filtered audio input.

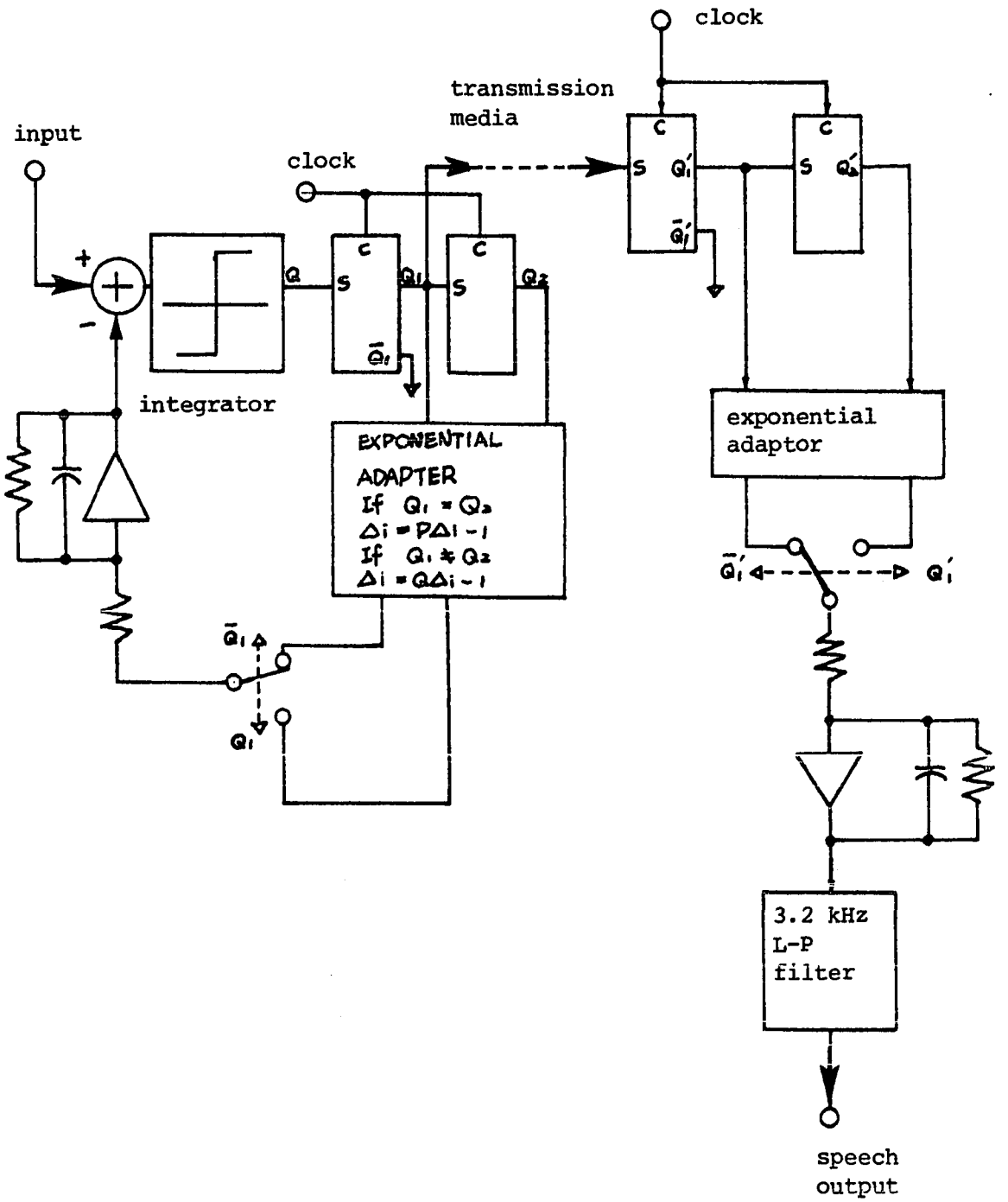

Figure 2.7. Jayant's ADM system

The adaptive scheme can be tabulated as follows:

Table 2.1. A table for Jayant's adaptive scheme

Sign of last two bits		Step sizes
11 or 00	$s_i = s_{i-1}$	$d_i = P \times d_{i-1}$
10 or 01	$s_i \neq s_{i-1}$	$d_i = Q \times d_{i-1}$

where

d_{i-1} is the previous step size

d_i is the present step size

3. Song's robust ADM system: [27] Song et al. used a mathematical approach to obtain an optimum scheme to give the least mean square error based on the two previous bits for Markov-Gaussian source signals. The nonlinear equations obtained for the theoretically optimum system are then reduced to piecewise linear equations and implemented. It turns out that the reduced results are similar to Jayant's with P = 1.15 and Q = .51 except that $P \times Q \neq 1$. Song's results were slightly inferior due to too many linearizing approximations to Gaussian distribution functions which were used in the analysis and inherent noise in A/D and D/A

converters which were employed for implementation, and the fact that speech signals are not exactly Markov-Gaussian source signals.

4. Daugherty's ADM system: [38] Daugherty's system is basically the same as other systems in the sense that it also uses multiplication factors. The adaptive scheme was developed by looking at computer plots and the output waveshapes of a simple delta modulator operating at a maximum S/N ratio. The ratio of the largest step size to the smallest step size is 48 dB. The ratio of adjacent step sizes is 6 dB. As is shown in Figure 2.8, he also inserted an integrator following the error signal between the original signal and the predicted signal.

5. Other systems which are basically similar to the previous systems can be found in the literature [1]. Zetterberg and Uddenfeldt [42] tried to investigate Jayant's ADM further for different P's and Q's with computer simulations. It appears that the relatively low S/N ratio is caused by a slight delay in the subtraction procedure for computing noise power and by an approximation of low-pass filter response. Abate [25] showed with computer simulations that somewhat improved performance could be achieved by subdividing the step sizes, i.e., considering more step sizes. It is understandable that discrete systems tend to work better for a rapidly changing signal than analog systems.

Table 2.2. A table for Daugherty's adaptive scheme

last change of level	decrease will occur on digits shown	increase will occur on digits shown
increase	1010 or 0101 (4 digits)	1111111 or 0000000 (7 digits)
decrease	1010101 or 0101010 (7 digits)	111 or 000 (3 digits)

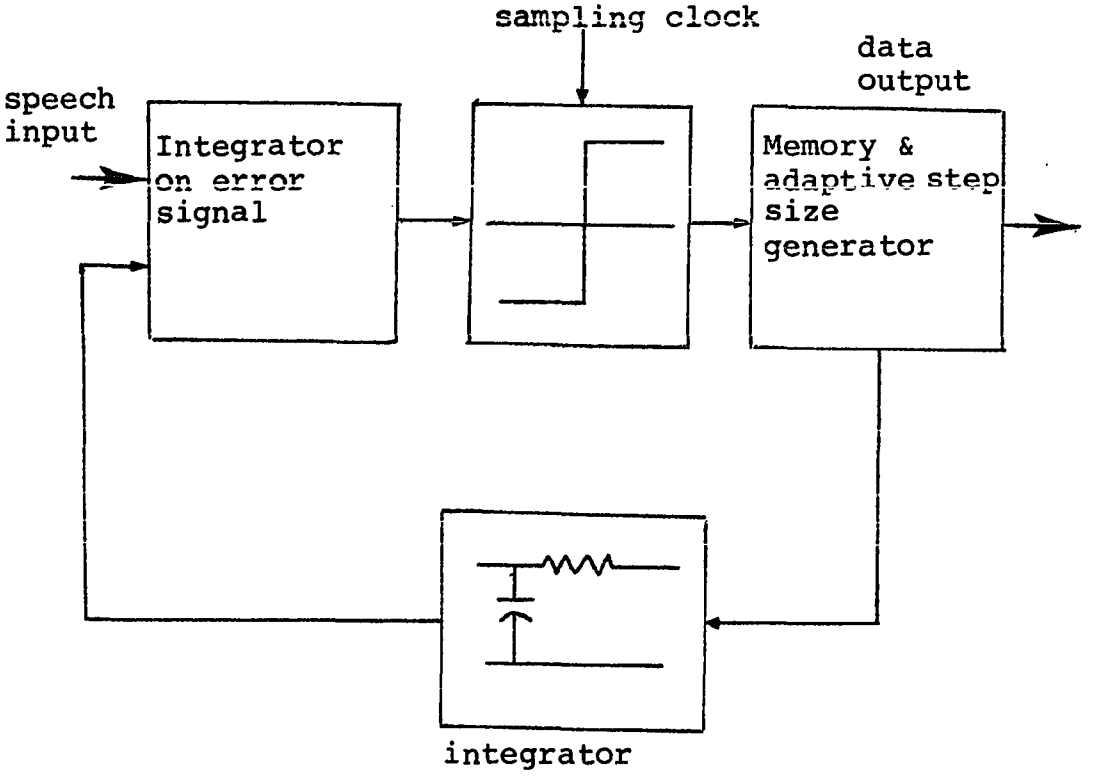

Figure 2.8. Daugherty's ADM system

One thing to note in comparing the system performances is that some variations in the S/N ratio of systems are observed due to different testing conditions.

3. A NEW ADAPTIVE DELTA MODULATION

3.1. Overview of the System

The motivation for the ADM system presented here comes from the following considerations: All the previously mentioned discrete systems largely consider either consecutiveness (11, 00) and alternation (10, 01) of the last two bits for the multiplication by P or Q, or extreme sequences like 010101., 111111., and 000000.... But in the system presented here "n" bits (n>2) are considered, which in consequence generate 2^n output sequences. The sequences which are not extreme, and which are associated with concave or convex patterns, are used for intermediate step sizes. Since the sampling frequency is usually many times greater than the input signal's bandwidth, there might be some wave patterns associated with specific bit strings whose corresponding optimum step sizes would give the least mean squared estimate of either a deterministic or stochastic signal. In other words, one wishes to minimize the mean squared error between a given input signal and an estimated signal based on "n" previous bits. Therefore the most important thing in such a system is to find optimum step sizes for the corresponding sequences.

The block diagram of the proposed ADM system is shown in Figure 3.1. Since we are assuming that the step sizes for

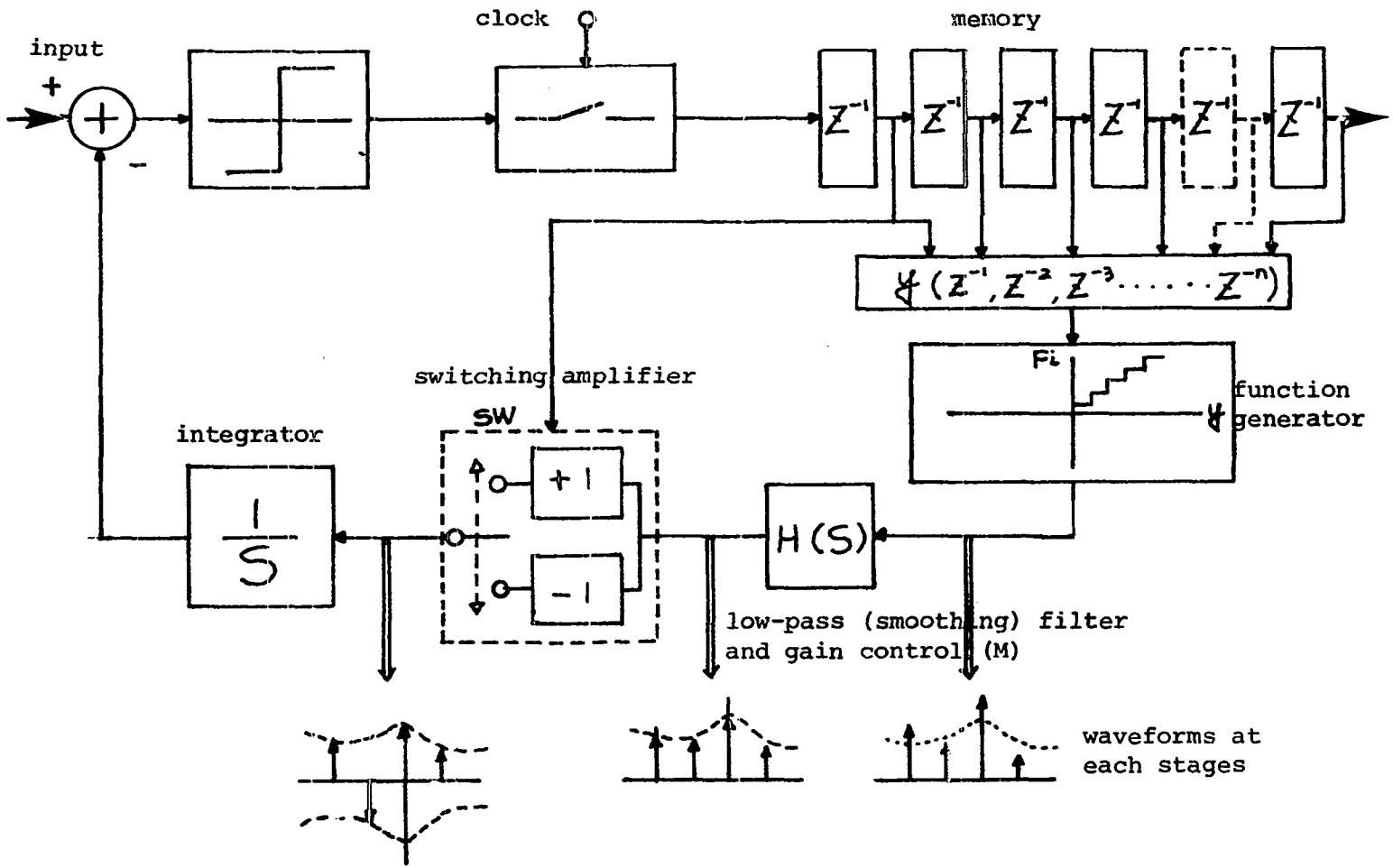

Figure 3.1. Block diagram of the proposed ADM

complementary sequences (1011 and 0100, 10101 and 01010, etc.) are the same magnitude, but opposite in polarity, steps of only one polarity are generated; the polarity is then reversed when required.

A mathematical description of the system is given in Appendix B.

The purpose of the low-pass (smoothing filter) filter following the step-size generator will be explained in the later chapters.

3.2. Hardware Implementation

It was decided that the proposed system be implemented and tested with a criterion of signal-to-noise ratio which is a much used measure in communication systems. A receiver was not built since it was a duplication of the feedback loop of the transmitter that was implemented. Instead, the output of the integrator was used as a test output.

The design of the proposed system is illustrated in Figure 3.2. First, a linear delta modulator was implemented and tested. The adaptive scheme was then added to the LDM.

The major blocks in the system shown in Figure 3.2 will now be explained in detail.

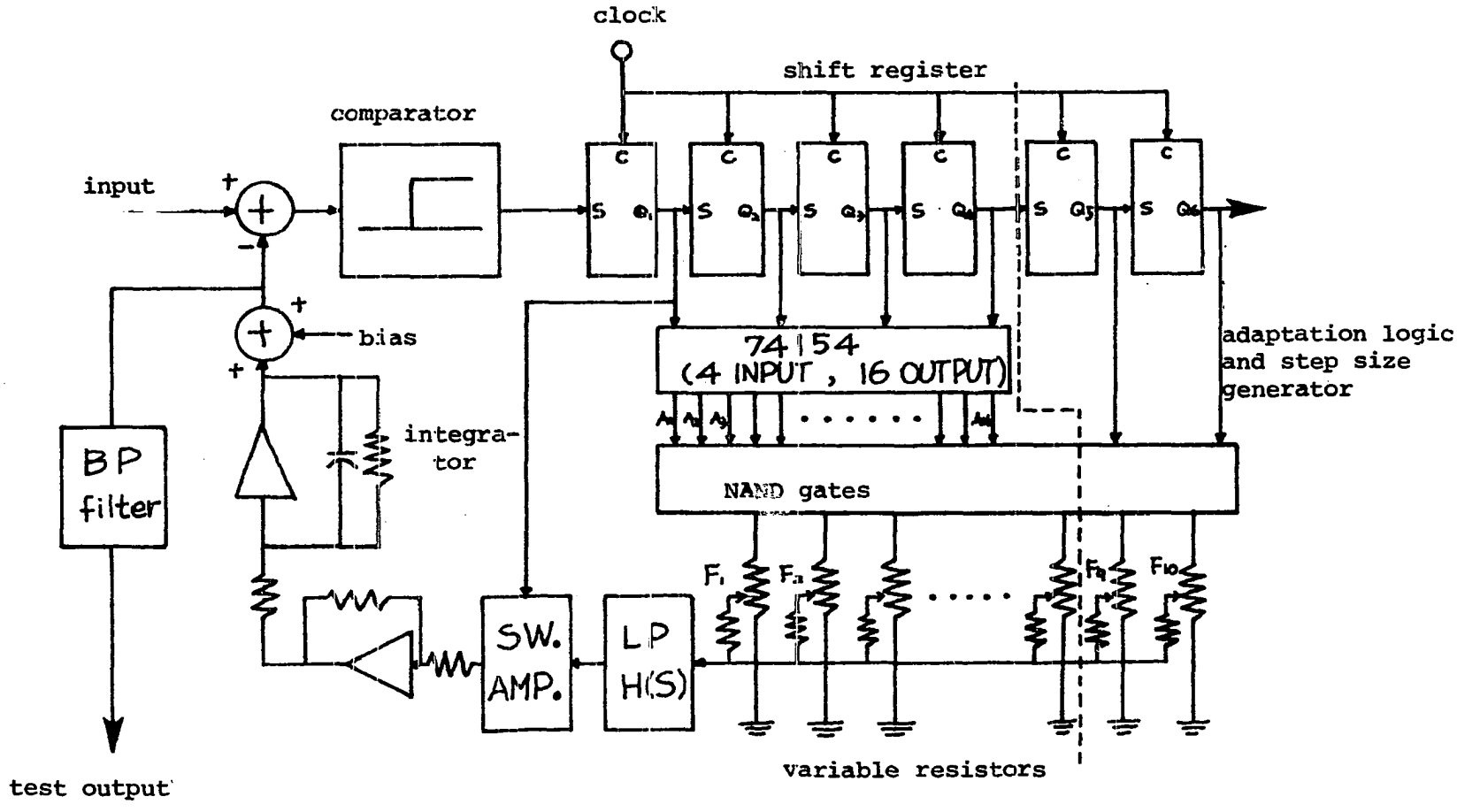

Figure 3.2. Description of the system

A. Comparator (SN72710):

It compares two inputs and yields 5 volts or 0 volts depending on which input is greater. (The complete circuit diagram of the comparator, the integrator, and the shift register portion is given in Figure 3.3).

B. Shift Register (DM7473):

The J-K flip-flops shown in Figure 3.2 works as memories. The shift register output is decoded by decoder (74154) later. It shifts contents of the previous bit to the next bit at each clocking instant.

C. Integrator:

A perfect integrator tends to be unstable due to an inevitable imbalance of positive and negative values of the decoding output, which may result in a d-c build up problem. So a 'leaky' integrator with a cutoff frequency at 175 Hz was built using an operational amplifier (LM301A) and the adjustment of d-c biasing is done by d-c level shifting.

Throughout the implementation 301A type operational amplifiers were used. One more advantage of the leaky integrator is that the transmission bit errors will tend to be stabilized. Otherwise the voltage generated by wrong bits may build up or saturate at the output of the integrator.

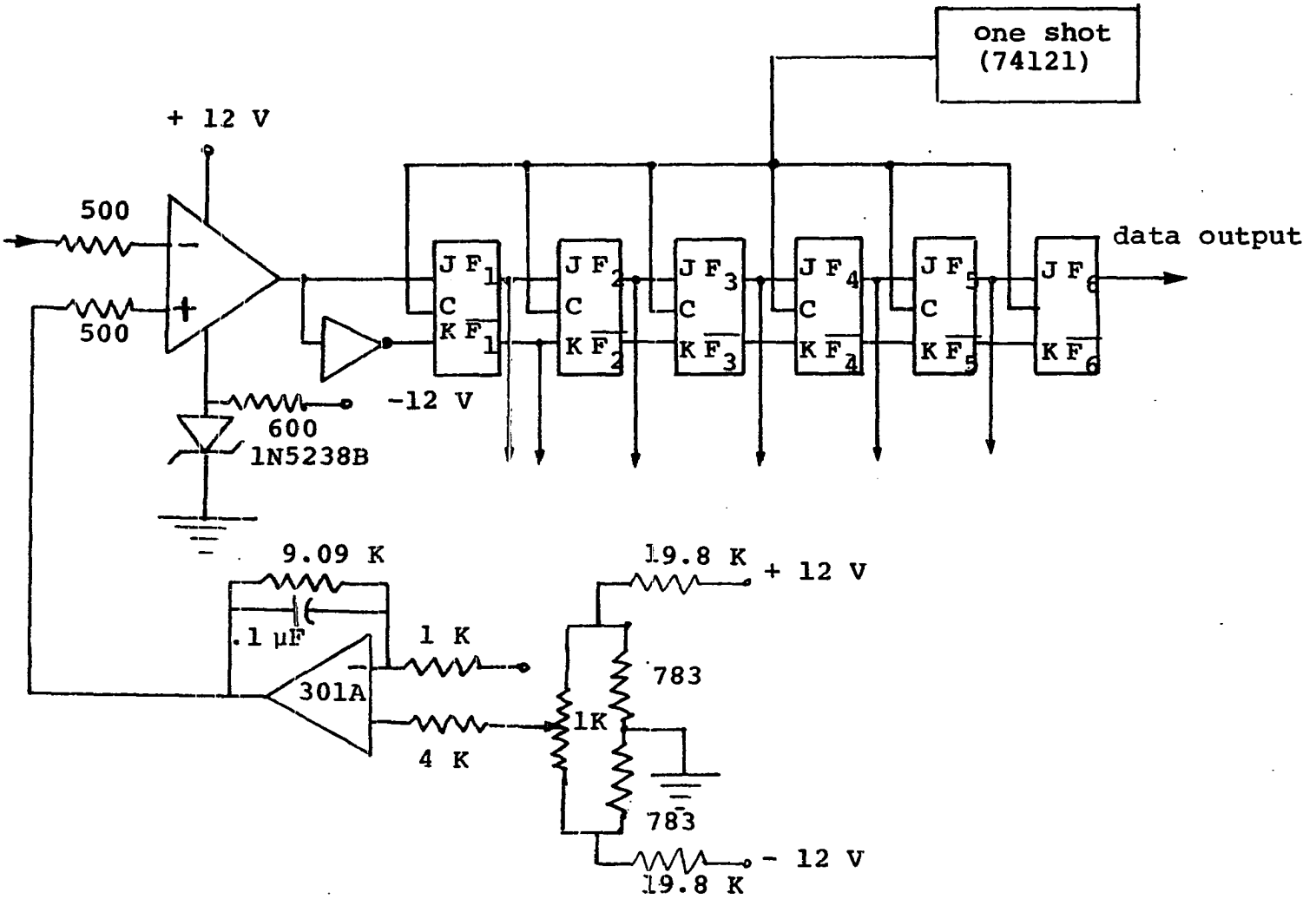

Figure 3.3. A circuit diagram of the comparator and the shift register and the integrator

D. Switching Amplifier:

Instead of generating opposite polarities for each step size with the same height individually, a simpler approach was taken. A switching amplifier whose output polarity can be controlled by the output of the last bit was built. For example, the sequence 1110 and its complement 0001 have the same amplitude only with opposite polarities.

An analysis of a switching amplifier is given below (Figure 3.4):

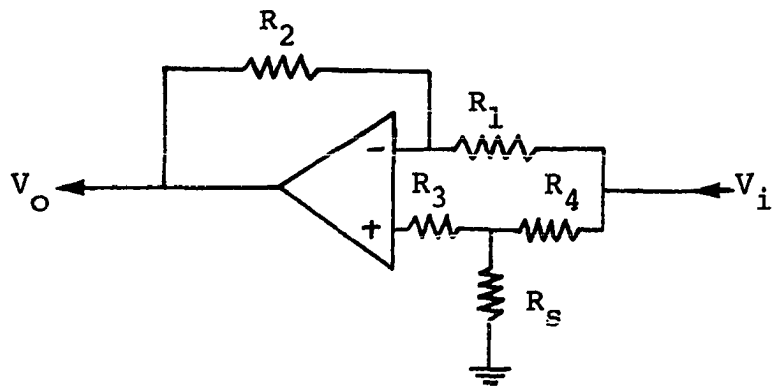

Figure 3.4. A simplified diagram of a switching amplifier

1. When $R_s = 0$

$$V_o = -\frac{R_2}{R_1} V_i = -V_i$$

when $R_1 = R_2$

2. When $R_s = \infty$

$$V_o = (\frac{R_1+R_2}{R_1})V_i - \frac{R_2}{R_1} V_i$$

$$= V_i$$

To control the variable resistor R_s by the output of the shift register, analog switches compatible with TTL family were chosen. The performance of these selected switches (IH5010N) was far from ideal beyond certain specified input levels. Therefore the performance of the switching amplifier was somewhat limited. When the input level is above 2.1 volts it does not produce the same heights with different signs, and when the level is below 40 mv, the output is more or less drifting from the zero level.

The complete circuit diagram of the switching amplifier is illustrated in Figure 3.5.

E. Step Size Generator (adaptive scheme):

A decoder with TTL logic gates to decode all possible output sequences was built. First, a way to generate appropriate voltages for corresponding sequences will be explained. A TTL 74154 (4 input 16 output) demultiplexer generates $2^4 = 16$ output sequences with 4 outputs from the shift register. A four bit code and its complement will produce the same height from the demultiplexer and NAND gates

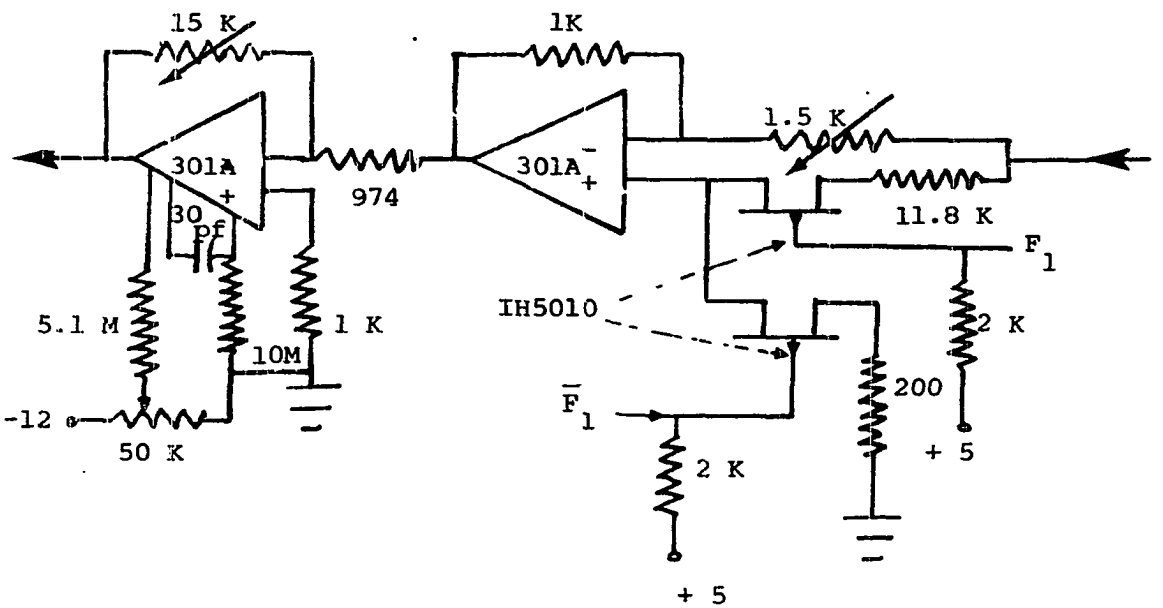

Figure 3.5. A complete circuit diagram of the switching amplifier and the offset voltage adjusting amplifier

configuration shown in Figure 3.6.

For the four extra sequences, 11111, 111111, 000000, and 00000, the sequences 1111 and 0000 are utilized. (The purpose of the four extra sequences is explained later.) The gates for the sequences (1111, 0000) are NANDed with the previous two bits. So whenever either 1111 or 0000 is

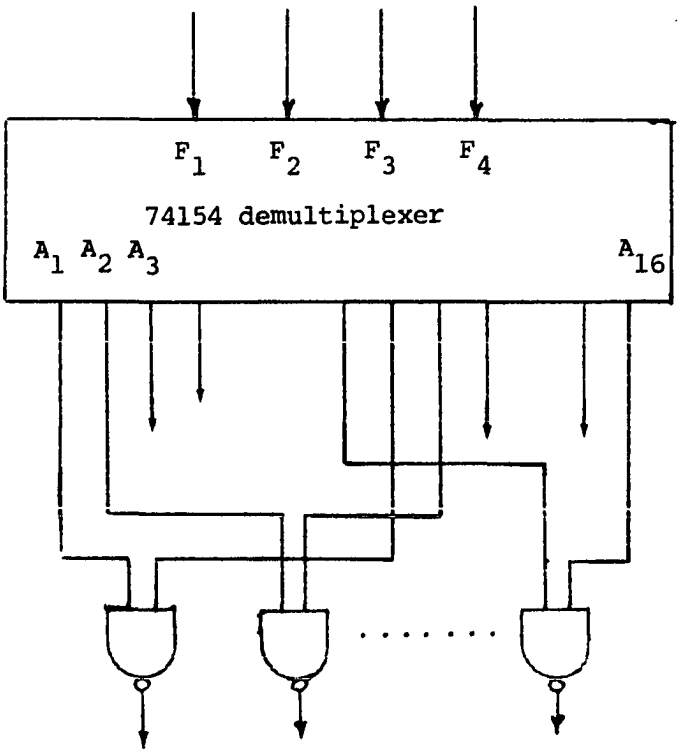

Figure 3.6. A circuit diagram for the 4 input 16 output output demultiplexer

generated, it automatically checks the signs of the previous two bits to see whether the signs are the same as with the four bits or not. Depending on the results of the checking the corresponding gates go high at each instant. If the signs are the same (111111, 000000), the gate for either

111111 or 000000 stays high. In a similar way other sequences are generated. This is shown with an example assuming we have a sequence like:

1 0 1 1 1 1 0 1 1 1 1 1 1 0 0 1 0 1 0

where the left-most digit represents the most recent output of the register. Then sequences with timing order and polarities as shown in Figure 3.7 are generated.

After decoding the sequences the output level may be either adjusted by a trimmable resistor connected between the gates and ground (Figure 3.8), or used for a TTL compatible analog switch in the feedback resistor (Figure 3.9) as will be detailed next. Two alternative ways to use these sequences for generating step sizes can be considered. One way is to use adjustable voltage drop across the output resistors of the logic gates as an input to an operational amplifier. It is illustrated in Figure 3.8. This method is simple but requires precision adjustment, since the high states of IC gates do not have exactly the same voltages.

Diodes were inserted between the output of the TTL gates and trimmable resistors to prevent small low state voltages of the other gates from contributing to the input of the operational amplifier.

Another way is to use analog multiplexers commercially

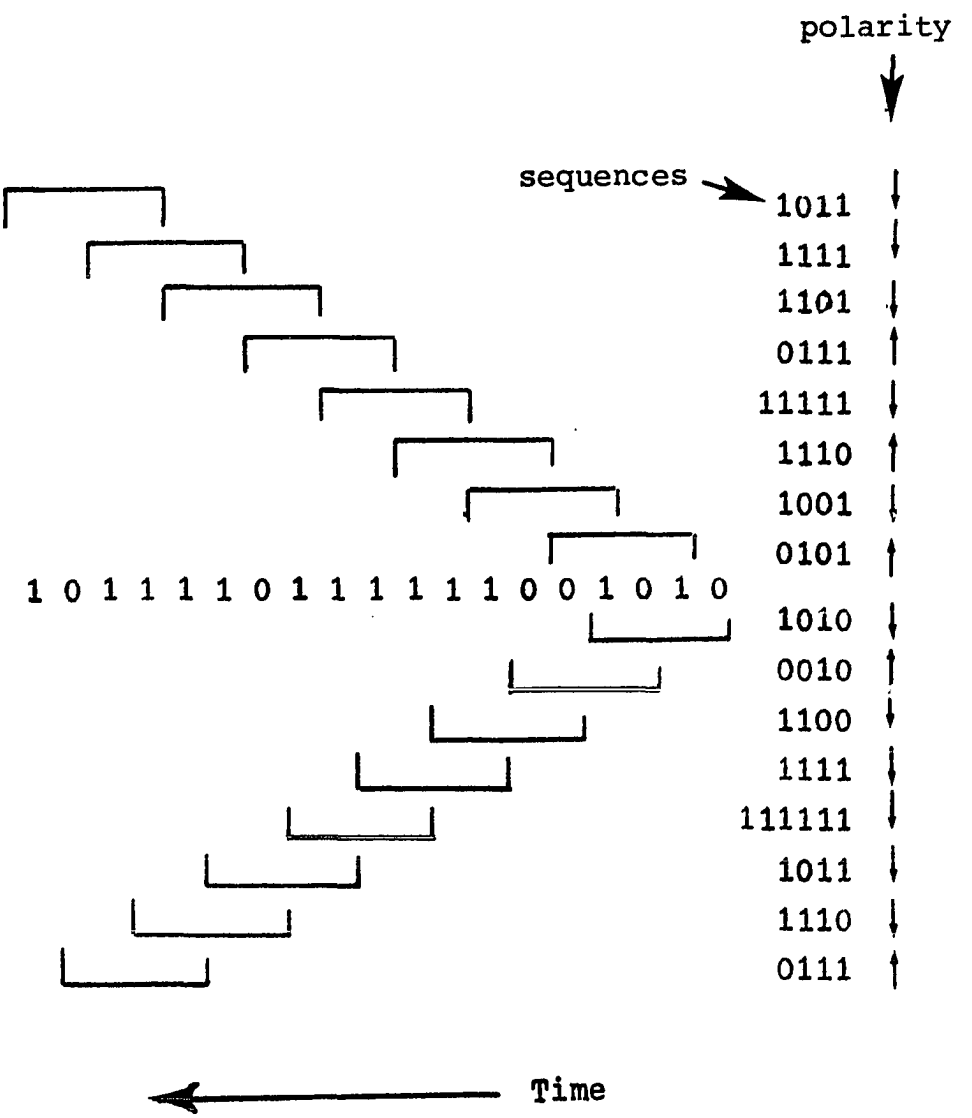

Figure 3.7. An example of the generated sequences

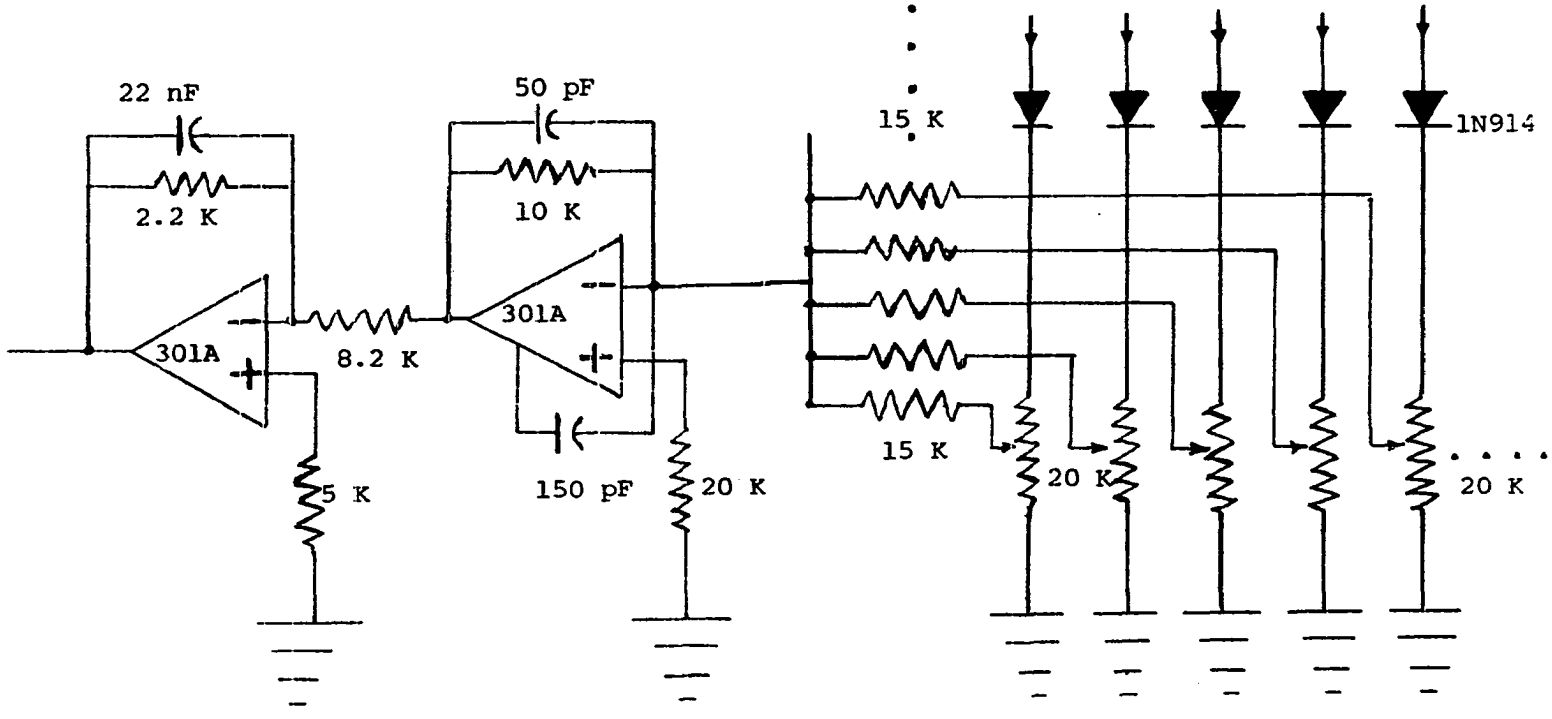

Figure 3.8. A circuit diagram of the step size adjuster and the low-pass filter

available and TTL compatible with IC chips. The Figure 3.9 is self-explanatory.

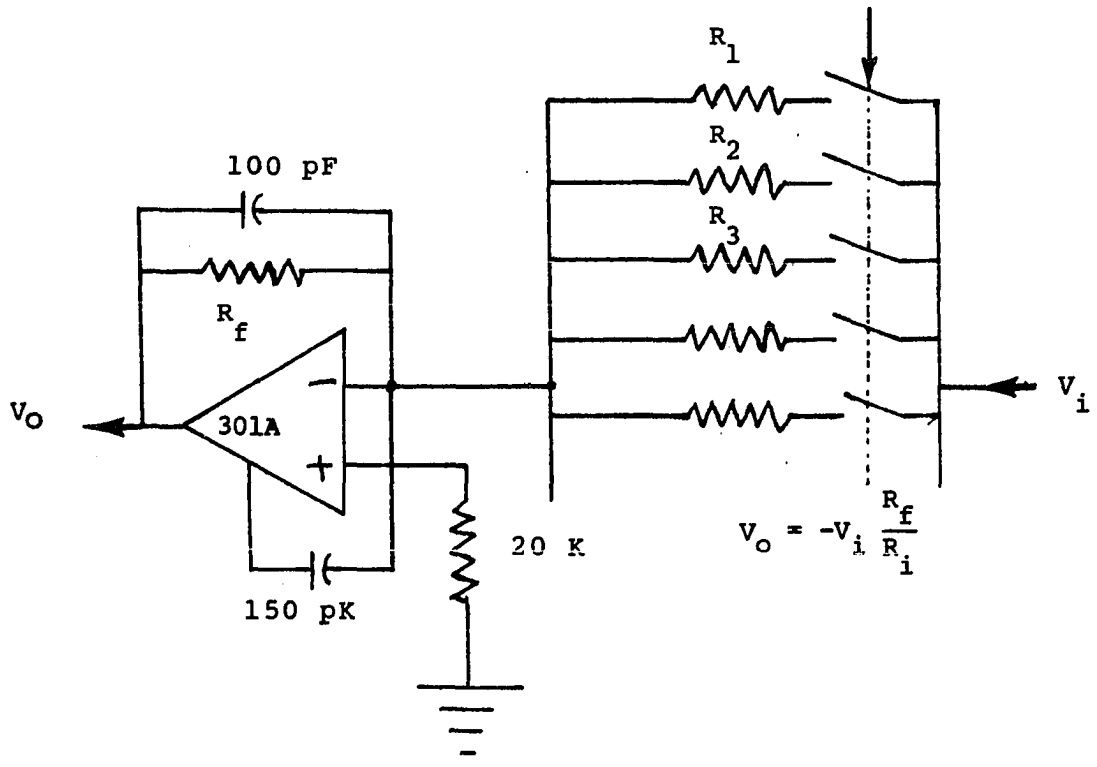

Figure 3.9. An alternative step size adjustor

The advantage of this scheme is that the previous fine adjustments are not critical as before, since the input voltage (V_i) remains the same. Due to economic reasons, the former approach was employed in the implementation.

F. The amplifier following the switching amplifier (Figure 3.5) was added to adjust the small d-c offset voltage of an operational amplifier which was critical for very small step sizes and to vary the scale factor by adjustable gain.

G. The bandpass filter in Figure 3.2 is explained in Chapter 4 in which the test procedure is described.

3.3. Determination of the Order of the Sequences

Considering the implementation problems, only four bit sequences (n=4) were considered initially. The 16 possible sequences are 0000, 0001, 0010, 1000, 1100, 1110, 1010, 1011, 1101, 1001, 1111, 0111, 0011, 0100, 0101, 0110. The problem of determining the order of these sequences is analyzed partly by following Jayant's idea. Using Jayant's approach, Table 3.1 can be derived (the most left bit is the most recent bit).

The table is interpreted in the following ways: From Jayant's method, when the two adjacent bits are the same, the multiplication factor is P, and when the two bits are different, it is Q. Since P>1 and Q<1, the order of the multiplied values is easily determined such as

$$P^3 > P^2Q > PQ^2 > Q^3.$$

Table 3.1. A table for determining the order of the sequences

Possible sequences	Multiplied values	Order
1111, 0000	P^3 (PPP)	1
1110, 0001	P^2Q (PPQ)	2
1100, 0011	P^2Q (PQP)	3 (4)[a]
1000, 0111	P^2Q (QPP)	4 (3)[a]
1101, 0010	PQ^2 (PQQ)	5
1001, 0110	PQ^2 (QPQ)	6
1011, 0100	PQ^2 (QQP)	7
1010, 0101	Q^3 (QQQ)	8

[a]The change of the order is interpreted later.

When the multiplied values are the same, we can weight the most recent multiplication factor more heavily. For example, P^2Q has the following order:

1110 (PPQ) > 1100 (PQP) > 1000 (QPP).

In the same way, for PQ^2 we also have:

1101 (PQQ) > 1001 (QPQ) > 1011 (QPQ).

Later we consider four more sequences 00000, 000000, 11111, 111111 to improve S/N ratio in the slope overlead

region at a minimal cost of granular noise without changing the systems too much. By considering the four added sequences the order of 1000 and 1100 is changed intuitively.

The meaning of some of the sequences will be explained:

1111 or 0000 - It indicates that the predicted output level is far above or below the input signal; i.e., large slope overload distortion has occurred. So the biggest step size available is necessary.

1010 or 0101 - The predicted digital output follows the input signal reasonably closely, so only granular noise is generated. To minimize this noise, the smallest step size is used.

1110 or 0001 - There exists a tendency to overload from the input signal, so an intermediate but rather big step size is necessary.

In similar ways, other sequences can be explained.

The possible waveforms associated with the specific bit string can be drawn as in Figure 3.10.

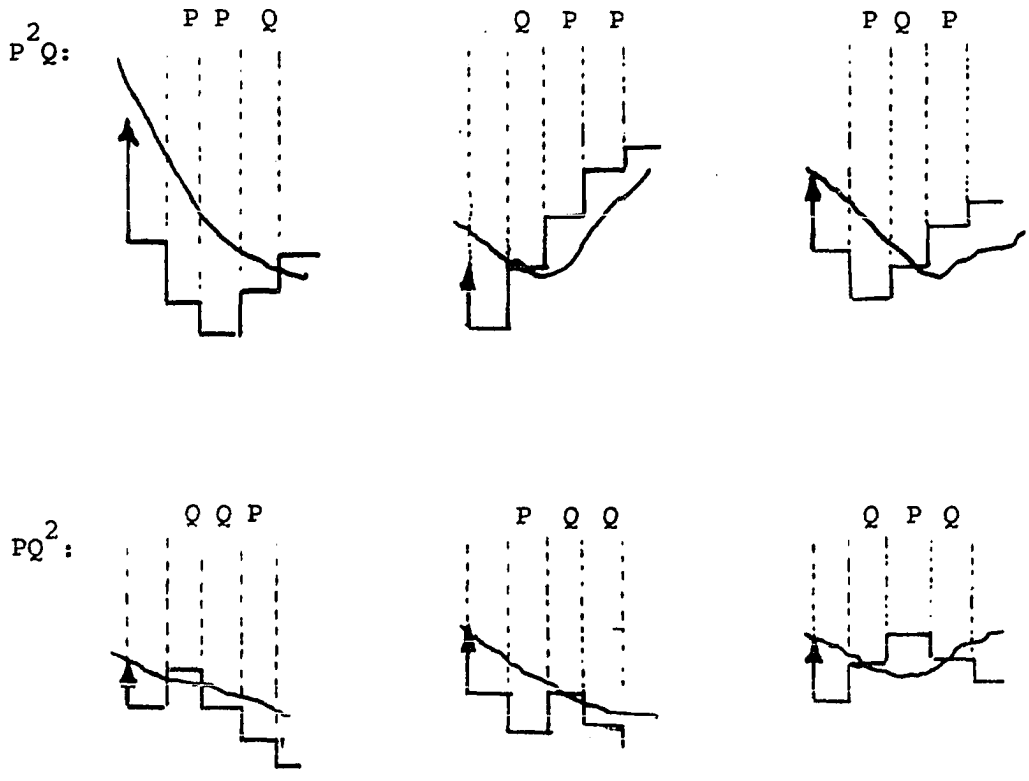

Figure 3.10. An example of bit strings

4. EXPERIMENTAL RESULTS

4.1. Test Procedure

A block diagram of the testing system is given in Figure 4.1. For low distortion in the input signals, an electron-tube type HP Wide Range Signal Generator Model 200CD was used. A slightly poorer performance was recorded with a signal generator which used a controllable flip-flop to generate a square waveform and then smoothed it with diode arrays.

There existed a slight delay between the sinusoidal input and the reproduced signal, so that the S/N ratio had to be measured with a distortion analyzer (HP Distortion Analyzer Model 330B), not by a subtractor between the two signals. Therefore slope overload noise measurements are not available, since a distortion analyzer can not record attenuation of the input signal.

The S/N ratio of the sinusoidal output from the signal generator was measured as 46 dB by the distortion analyzer.

As in telephone channels, the reproduced signals were band-pass filtered between 220 Hz and 3250 Hz with a Krohn-Hite Model 3100 filter set at a maximally flat response.

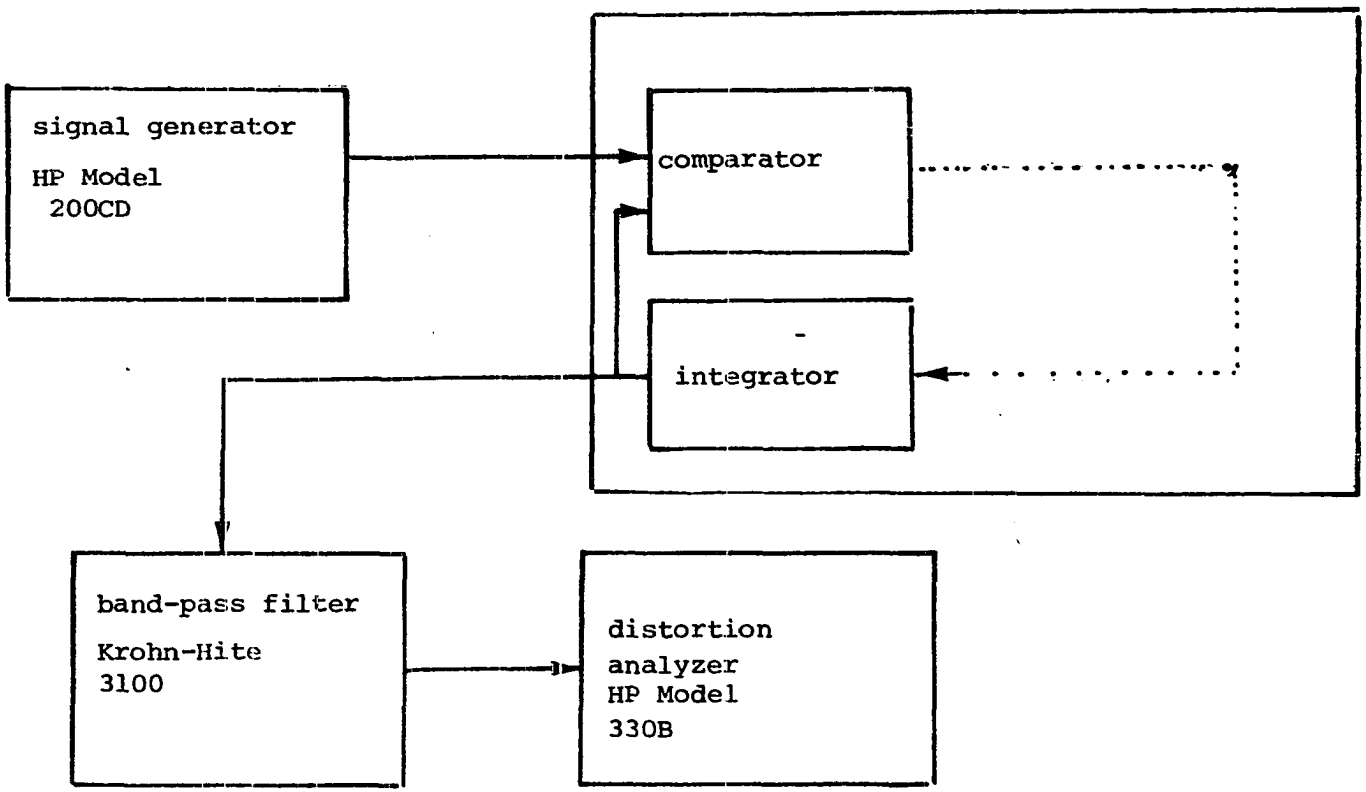

Figure 4.1. A block diagram of the testing system

4.2. Signal-to-Noise Ratio Measurements

Though it was pointed out [16, 43, 44] that the testing with S/N ratio performance criterion is not always best, it is still widely used in comparisons of digital modulators in communication systems. So the S/N ratio for sinusoidal input was chosen as performance criterion.

In choosing a test quantizer Paez's results of an exponential form were utilized first. The way of deriving optimum quantizers in PCM for different probability functions is treated in Appendix A. There exists no solid ground for using the Paez's results. Paez's quantizer was chosen since it was of an exponential form like most other quantizers, and it would be better than to start by guessing. In the process of experimentation other quantizers were treated.

A. The first test (quantizer No. 1, Fig. 4.6) with the Paez's result was made both with and without the low-pass (smoothing) filter whose cutoff frequency was set at 3.29 kHz. The input signal was an 800 Hz sinusoidal waveform, sampled at 56 kHz and 35 kHz separately.

The relative height of the sequence 1000 (or 0111) was given special attention. The sequences can be generated by overshooting after successive 1's or 0's. The number of the succession ranges from six to three in the adaptive scheme. After considering the possibility of 1000000,

100000 (or 0111111, 011111), the height of the sequence 1000 (or 0111) was allowed a higher value than it might be. The above rationale explains the sudden jump of the quantizer No. 1 in Figure 4.6.

Due to hardware limitations of the switching amplifier, the ratio of the largest to the smallest step sizes was limited to 43 = 32.6 dB.

As was expected, the low-pass (smoothing) filter in the feedback loop of the system smoothed out sudden changes in step sizes for very low input levels. Sudden changes in step sizes are very unlikely with continuous signals (Figure 4.2, 4.3, 4.4, and 4.5). These sudden changes in step sizes are the main cause of severe granular noise. Therefore S/N ratio is improved significantly with the low-pass filter. For relatively small signals this improvement is much larger than for big signals, because small signals are affected more by sudden step size variations. The results were plotted in Figure 4.7.

With the low-pass filter in the feedback loop, the adaptive technique in the proposed system can be regarded as a combination of a syllabic companding technique of a continuous ADM and an instantaneous companding technique of a discrete ADM. The degree of incline on either one is dependent upon the cutoff frequency of the filter. The lower the cutoff frequency is, the closer is the adaptation to a

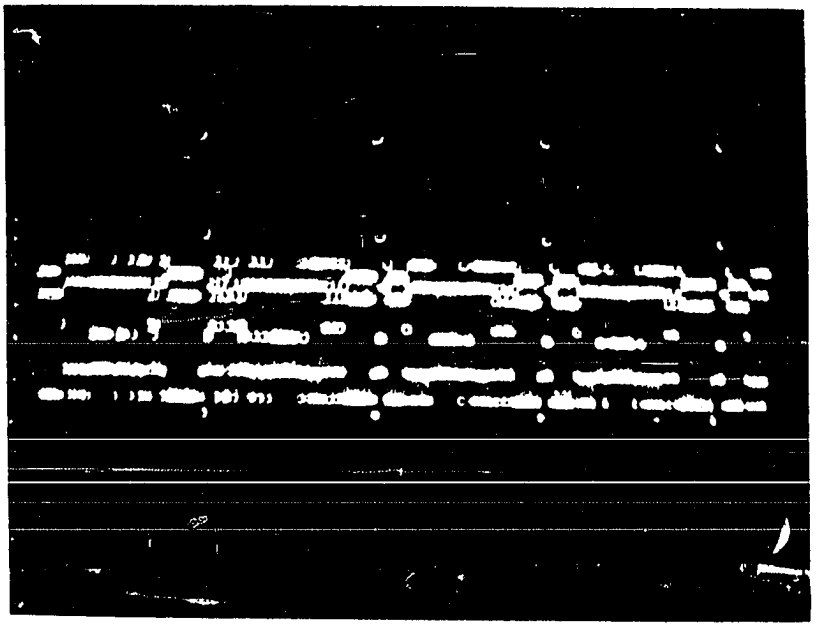

Figure 4.2. Instantaneous step sizes without the low-pass filter

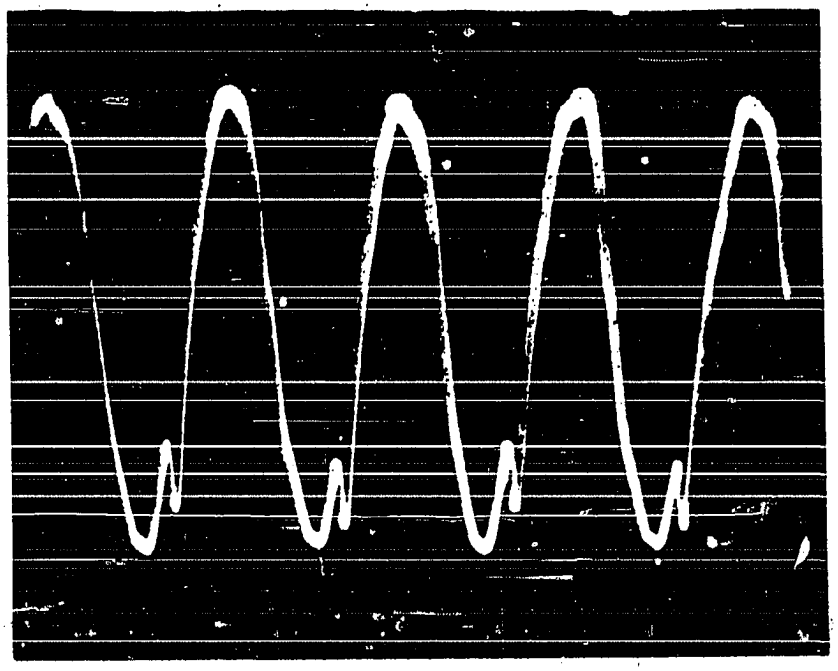

Figure 4.3. The reproduced output waveform through a band-pass filter between 220 Hz and 3,250 Hz (without the low-pass filter). Input frequency was 450 Hz

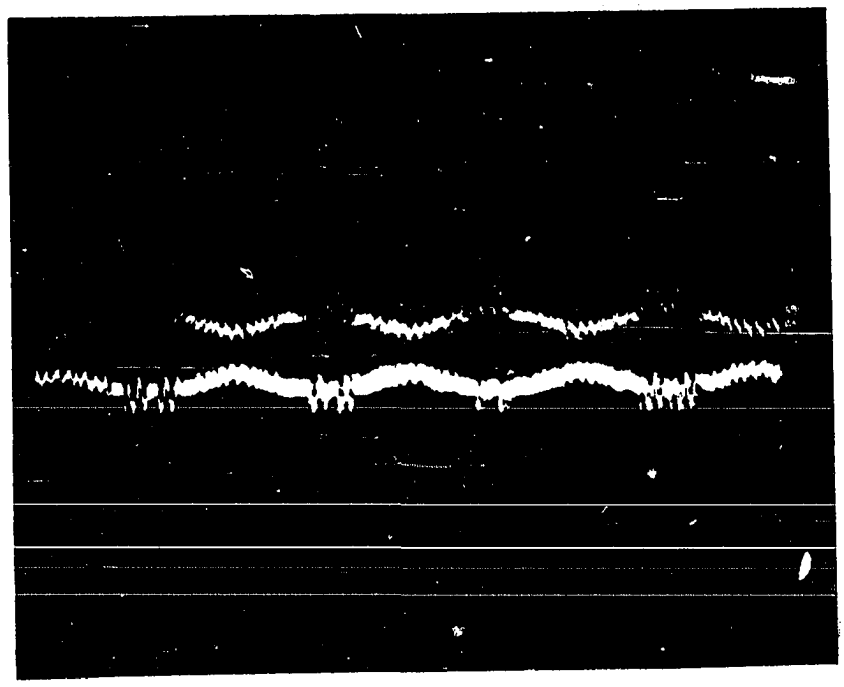

Figure 4.4. Instantaneous step sizes with the low-pass filter

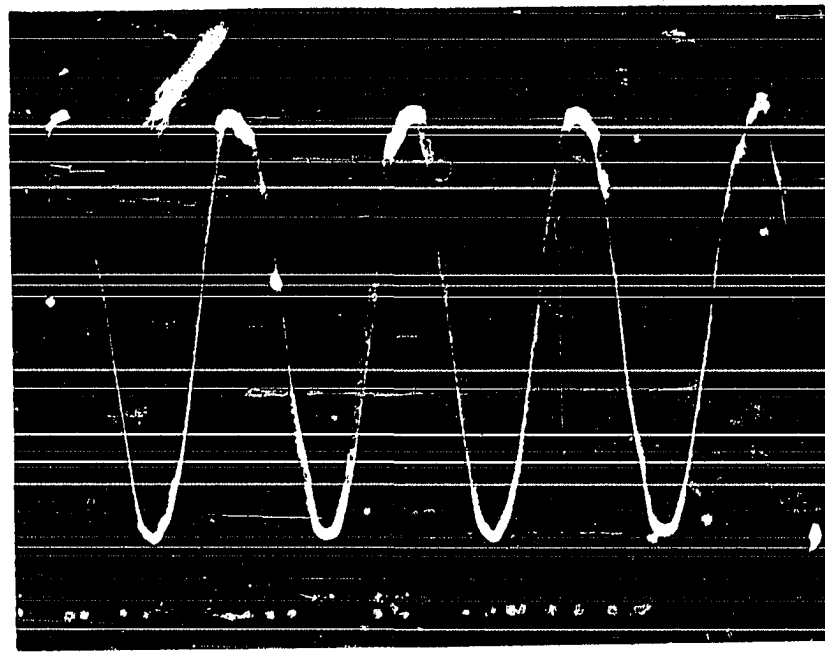

Figure 4.5. The reproduced output waveform through a band-pass filter between 220 Hz and 3,250 Hz (with the low-pass filter). Input frequency was 450 Hz

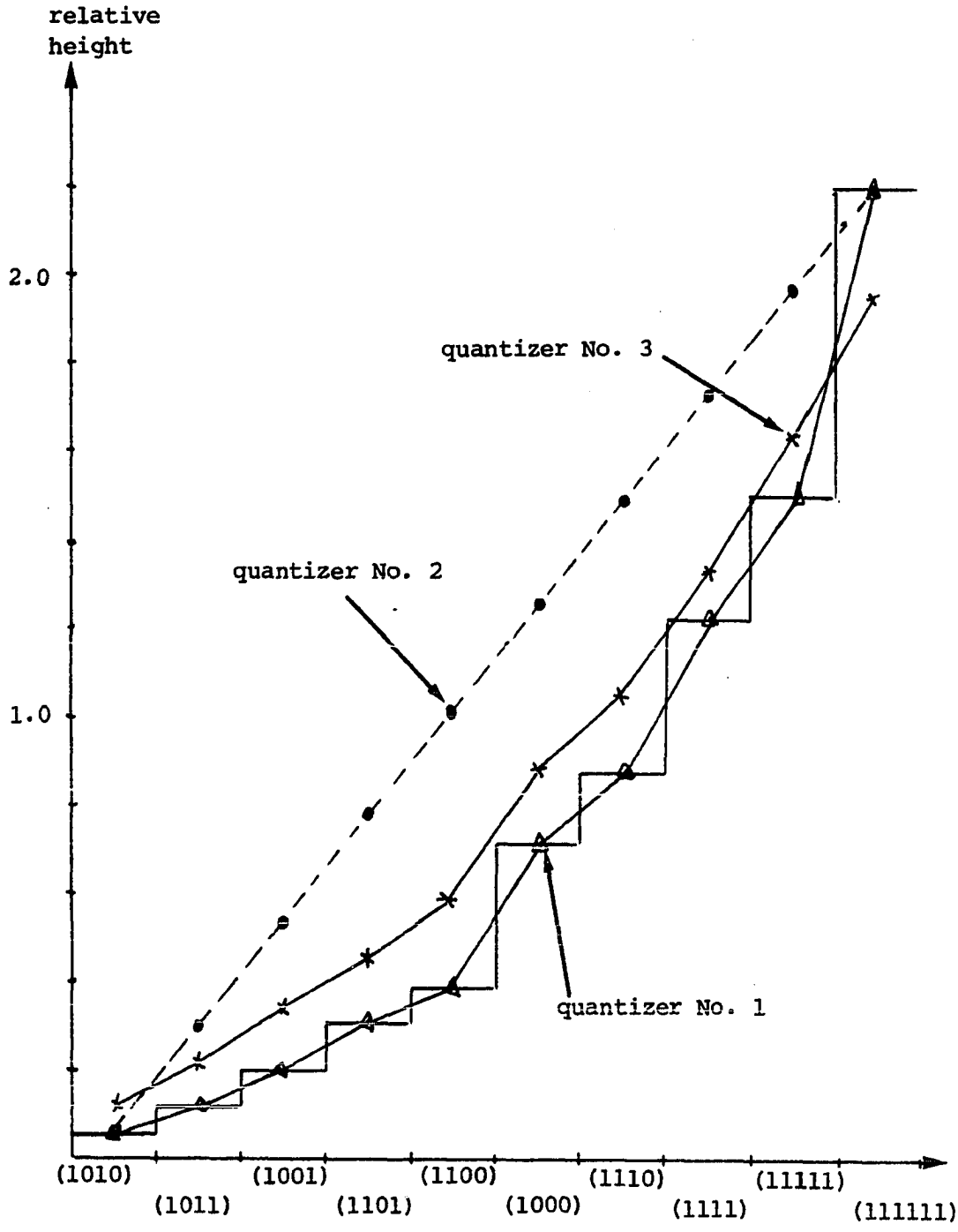

Figure 4.6. The relative heights of the sequence for 3 quantizers

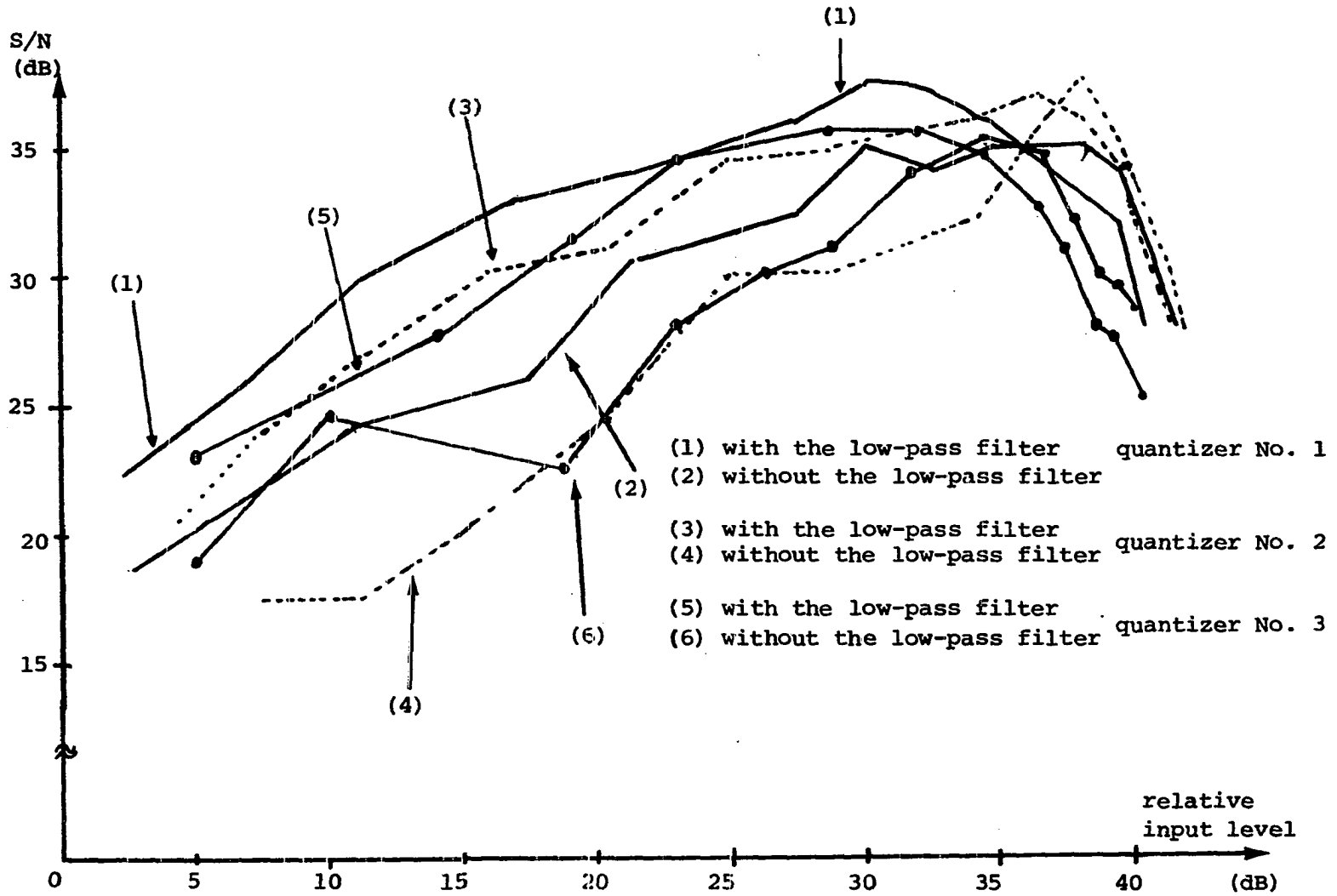

Figure 4.7. S/N curves for 800 Hz sinusoidal inputs sampled at 56 kHz

syllabic companding technique.

B. The second test was made with a uniform quantizer with the ratio of the largest to the smallest step sizes kept the same as for the No. 1 quantizer (see quantizer No. 2, Figure 4.6). The results are shown in Figure 4.7.

C. The third test was made with a quantizer an approximately exponential form (quantizer No. 3, Figure 4.6). In this case the ratio was only 19 = 25.6 dB. As is shown in Figure 4.7, some deterioration in S/N ratio for low level inputs is observed, and a more severe granular noise region than with the other two quantizers is found.

4.3. Observations

A. For extremely small signals, the S/N ratio is very sensitive to the threshold level of the comparator (710 type) which is controlled by trimpot.

B. Only low level step sizes are activated for small signals (Figure 4.9).

C. For medium level signals, all the step sizes are activated (Figure 4.10).

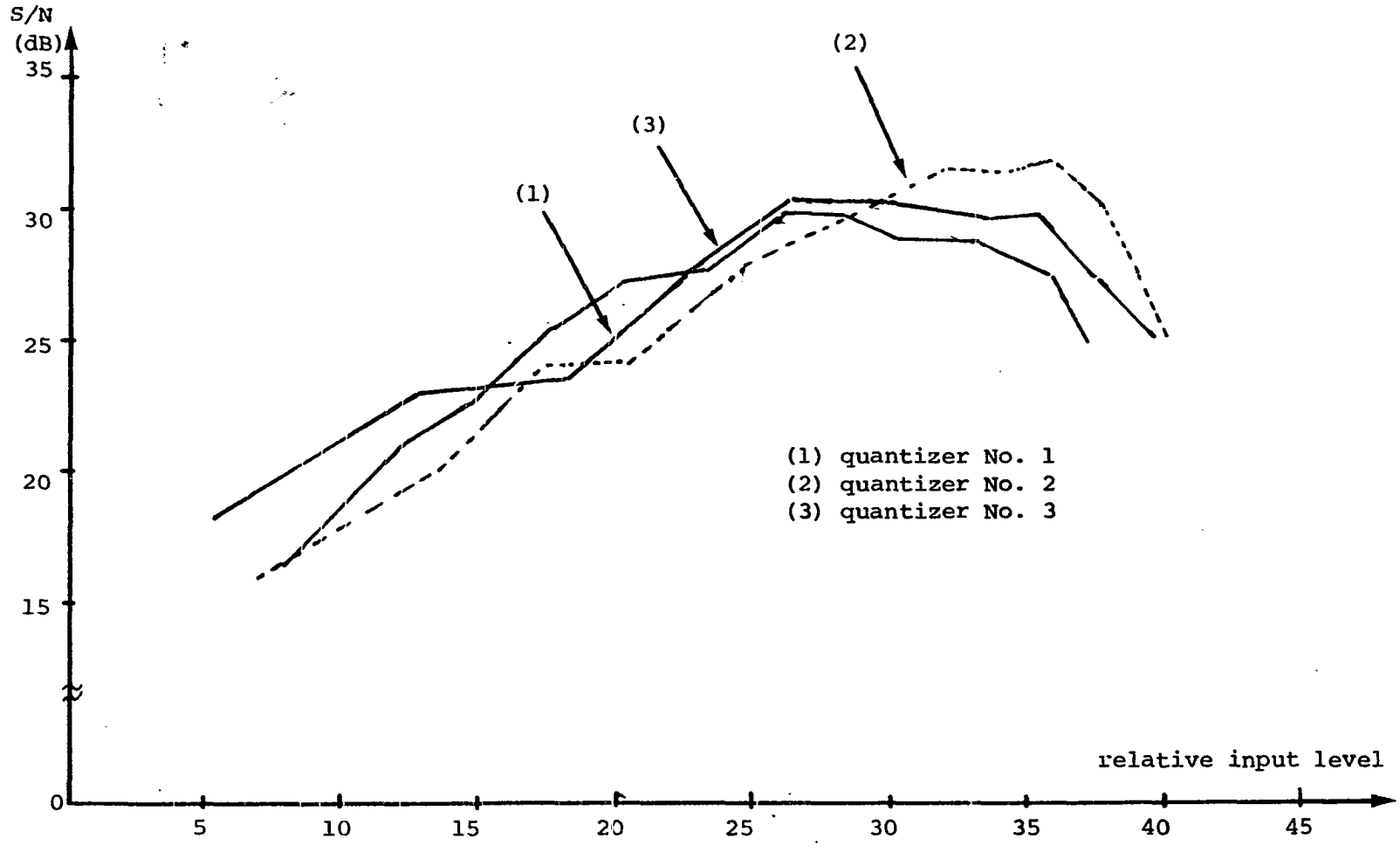

Figure 4.8. S/N curves for 800 Hz sinusoidal inputs sampled at 35 kHz (with the low-pass filter)

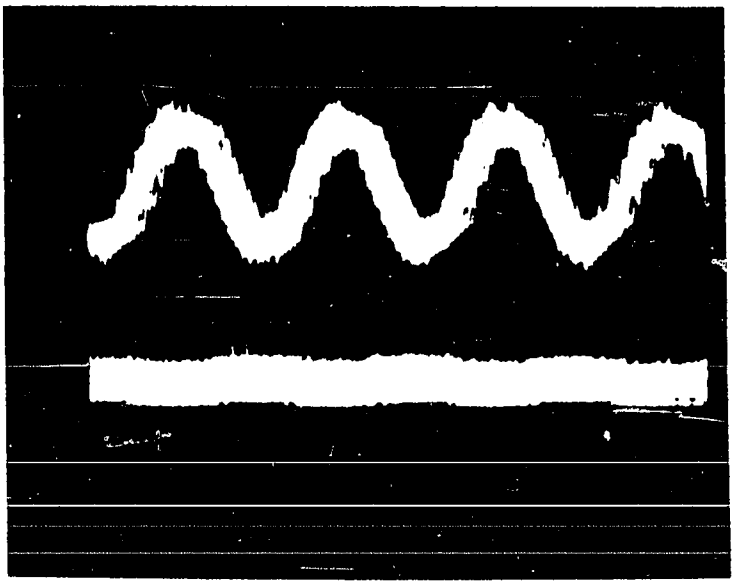

Figure 4.9. A reconstructed waveform and corresponding step sizes for small input level (without the low-pass filter)

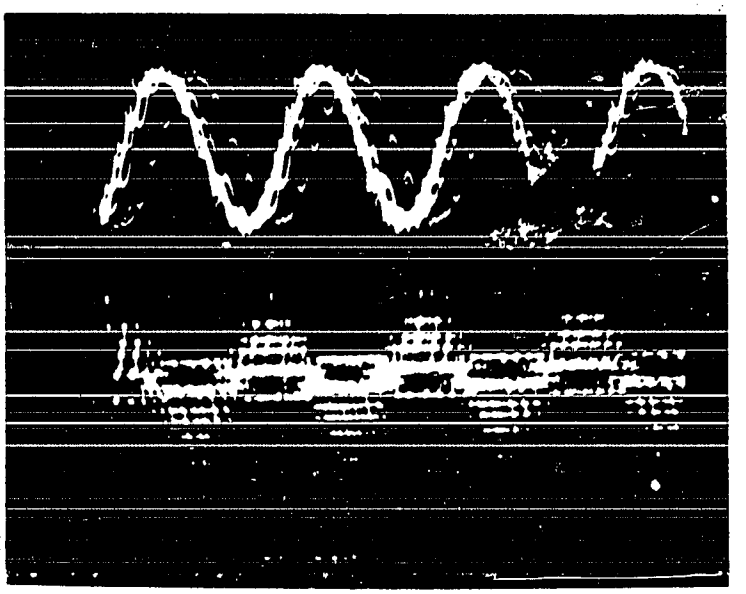

Figure 4.10. A reconstructed waveform and its corresponding step sizes for medium input level (without the low-pass filter)

D. For extremely large signals, the biggest step sizes are most often used, which in turn implies that slope overloading is occurring (Figure 4.11).

E. By lowering the sampling frequency from 56 kHz to 35 kHz, the S/N ratio is decreased by approximately 8-10 dB. This can be seen by comparing corresponding curves in Figure 4.7 and 4.8.

F. For medium level signals, the low-pass filter also smoothed out some granularity, so better S/N is achieved.

G. For extremely large signals, the low-pass filter causes a slight degradation in S/N ratio, because it slows sudden step size changes as shown in Figure 4.7. Figures 4.12 and 4.13 show the step sizes with and without the low-pass filter.

H. One more advantage related to the low-pass filter is that S/N curves are smoother, not fluctuating as they did without the filter.

I. By comparing those S/N curves of the three quantizers (Figure 4.7), it should be intuitively clear that quantizer No. 1 with the low-pass filter is somewhat superior to others. But one quantitative comparison, though not always used, that we are trying to make here is to compare the input-level range where the S/N ratio is over 30 dB

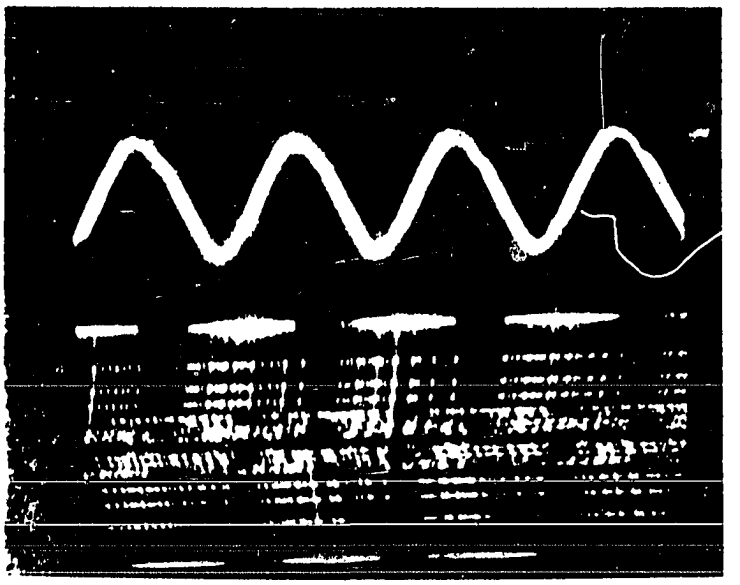

Figure 4.11. A reconstructed waveform and its corresponding step sizes for large input level (without the low-pass filter)

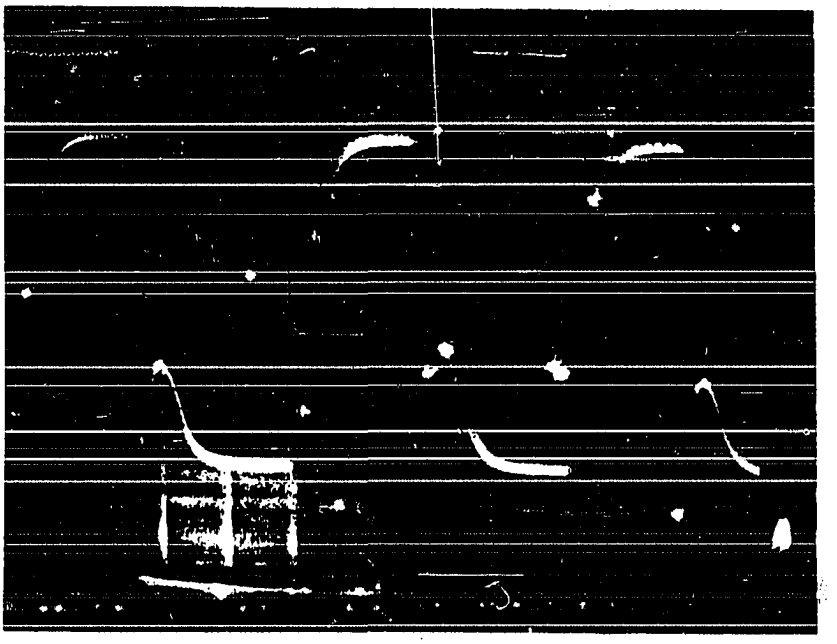

Figure 4.12. The instantaneous step sizes with the low-pass filter for large input level

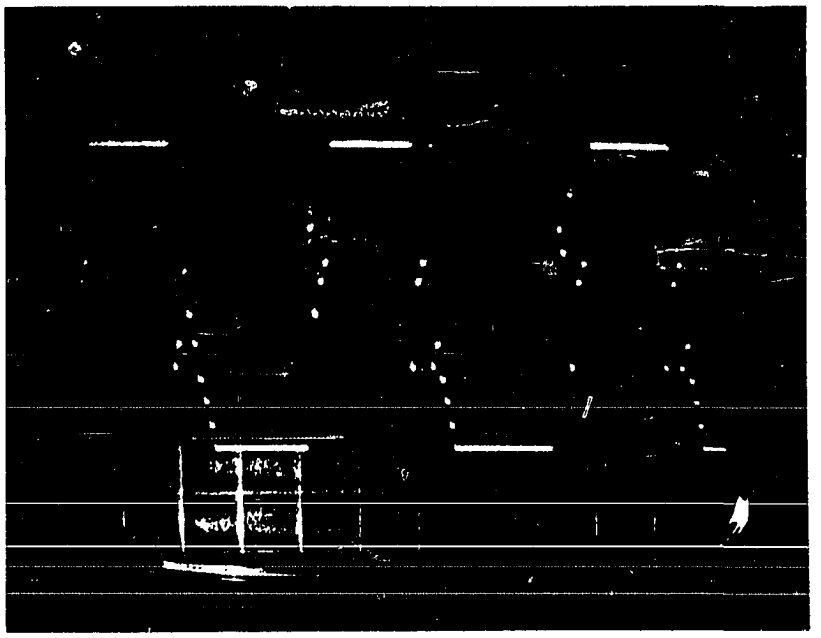

Figure 4.13. The instantaneous step sizes without the low-pass filter for large input level

(with the low-pass filter) for a sampling frequency of 56 kHz, and where a S/N ratio is over 25 dB (with the filter) for a sampling frequency of 35 kHz. The comparison is tabulated in Table 4.1.

Table 4.1 shows that quantizer No. 1 permits the widest input range at a sampling rate of 56 kHz.

J. By decreasing the gain of the amplifier following the switching amplifier by a factor of 1.7, a narrower dynamic range and a slightly inferior performance was observed (Figure 4.14), while the S/N curve was moved to the left.

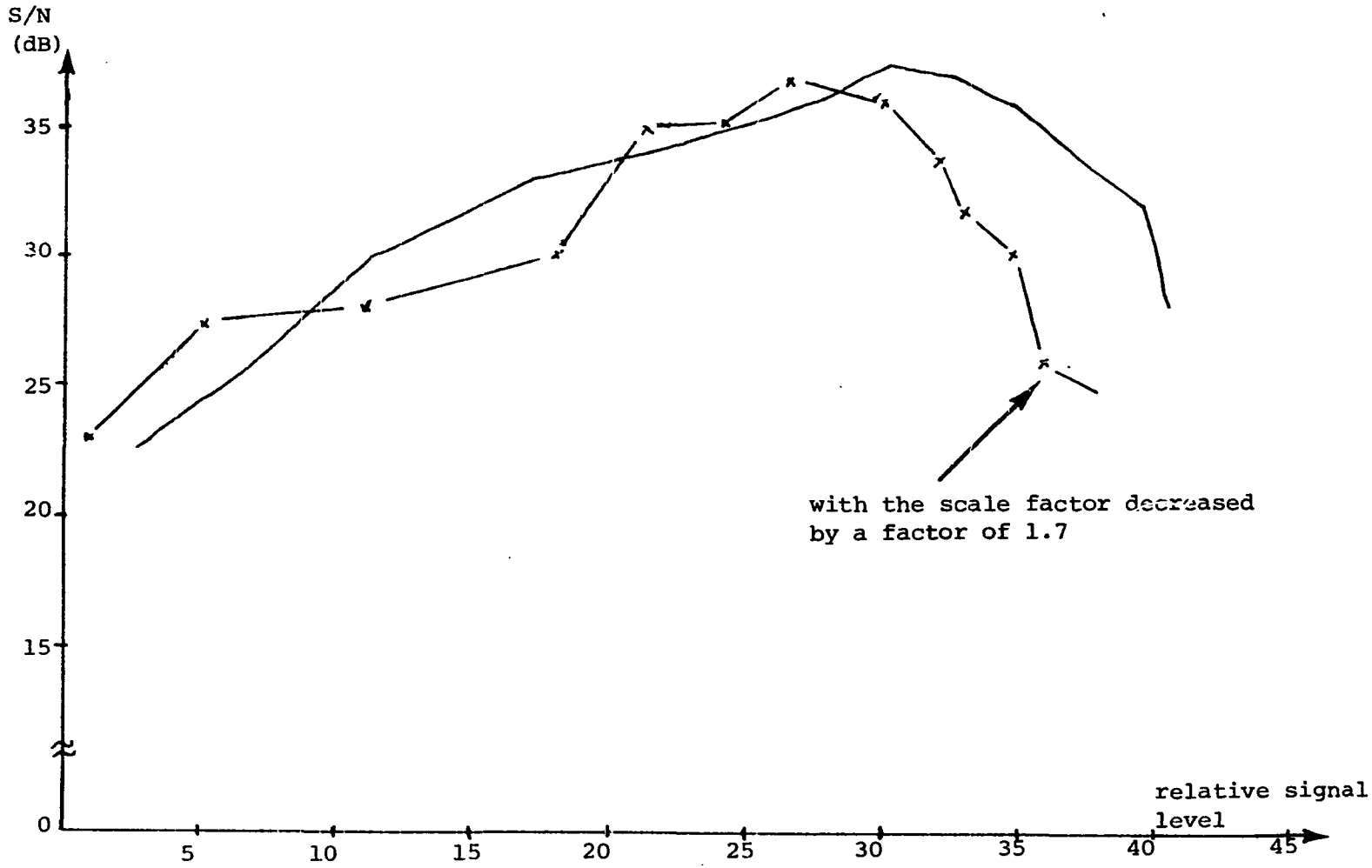

Figure 4.14. A comparison of S/N ratio with different scale factors

Table 4.1. Input-level range for 3 different quantizers with sampling frequencies of 35 kHz, 56 kHz

	Sampling Frequency	
	35 kHa	56 kHz
quantizer No. 1	19 dB	29 dB
No. 2	17.5 dB	25 dB
No. 3	19.5 dB	20 dB

K. The capacitor of the low-pass filter used was chosen so that it gave best performance out of 4 capacitors tried

L. Noises encountered in the experiment were removed by adding electrolytic by-pass capacitors between the d-c supplies of the operational amplifiers and the ground.

4.4. Comparisons with Other Published Results

Only a few S/N ratio curves for 800 Hz inputs, where data is based upon actual measurements on digital modulation systems, are cited in the literature. Majority of curves were computed by computer simulation for either sinusoidal waveforms or random signals with a known probability distribution.

Though it is not a simple matter to make a fair comparison with other systems based on published results with varying assumptions, comparisons with published S/N curves

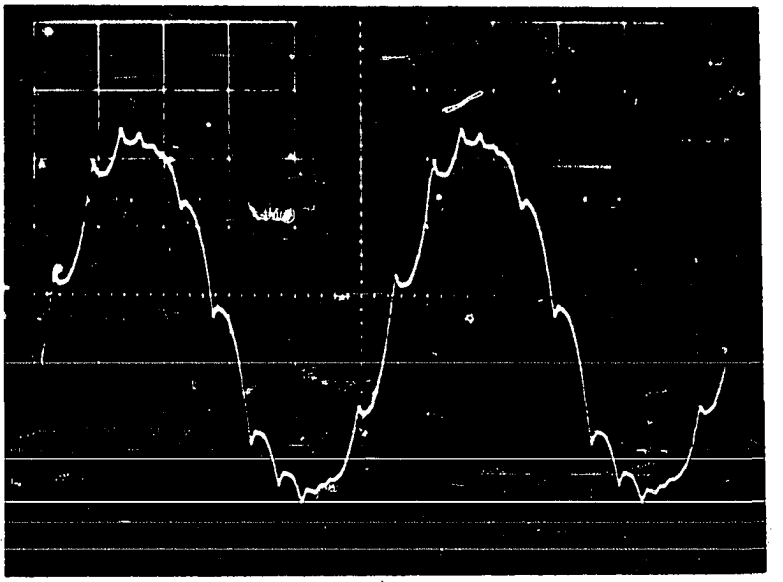

Figure 4.15. A typical reconstructed waveform of the ADM

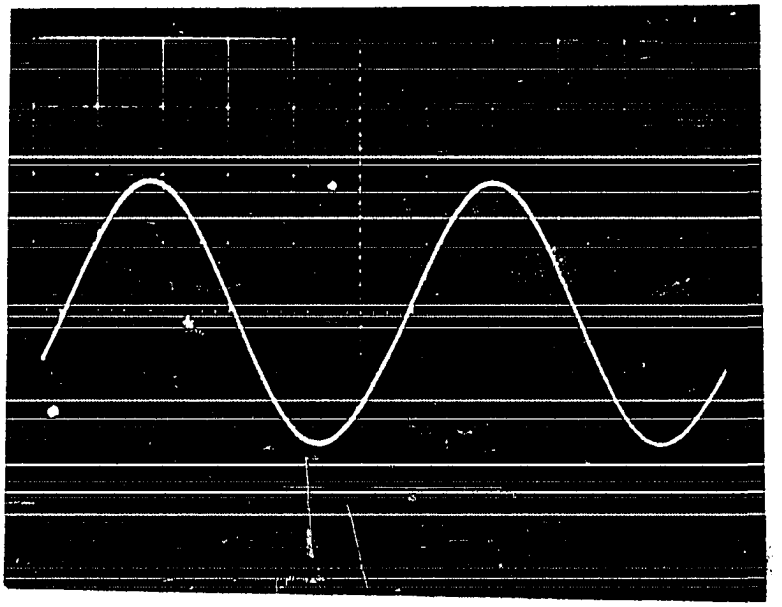

Figure 4.16. A band-pass filtered waveform

of other ADM schemes and of theoretical PCM system with A-law companding are made (Figure 4.17). The S/N curves of the new ADM system presented here are recorded for 800 Hz sinusoidal waveform with a sampling frequency of 56 kHz. As is shown in Figure 4.17, the performance of the ADM system is substantially better than that of Song's system and is somewhat inferior to that of Schindler's published result. The curves demonstrate a narrower dynamic range and a slightly higher peak (38 dB) in S/N ratio than Daugherty's system which was measured at 57.2 kHz. One thing to note in the comparison with Daugherty's system is that the ratio of largest to the smallest step size is 48 dB = 251 for Daugherty's system, whereas for the ADM system presented here the ratio is only 43 = 32.6 dB due to a limitation in the switching amplifier. The S/N curve also shows a comparable performance to a theoretical PCM system with 56 k bits. The comparison with other published ADM system S/N curve in the Schindler's paper [1] shows a superior performance of the ADM system presented here.

It is interesting to note that the S/N ratio curve of PCM system for real speech signals given by Schindler [45] is somewhat similar to the S/N ratio curve measured with 800 Hz sinusoidal waveform [1].

Curves (1), (3) and (6) recorded with 800 Hz sinusoidal waveforms are given in the literature [1] by Schindler.

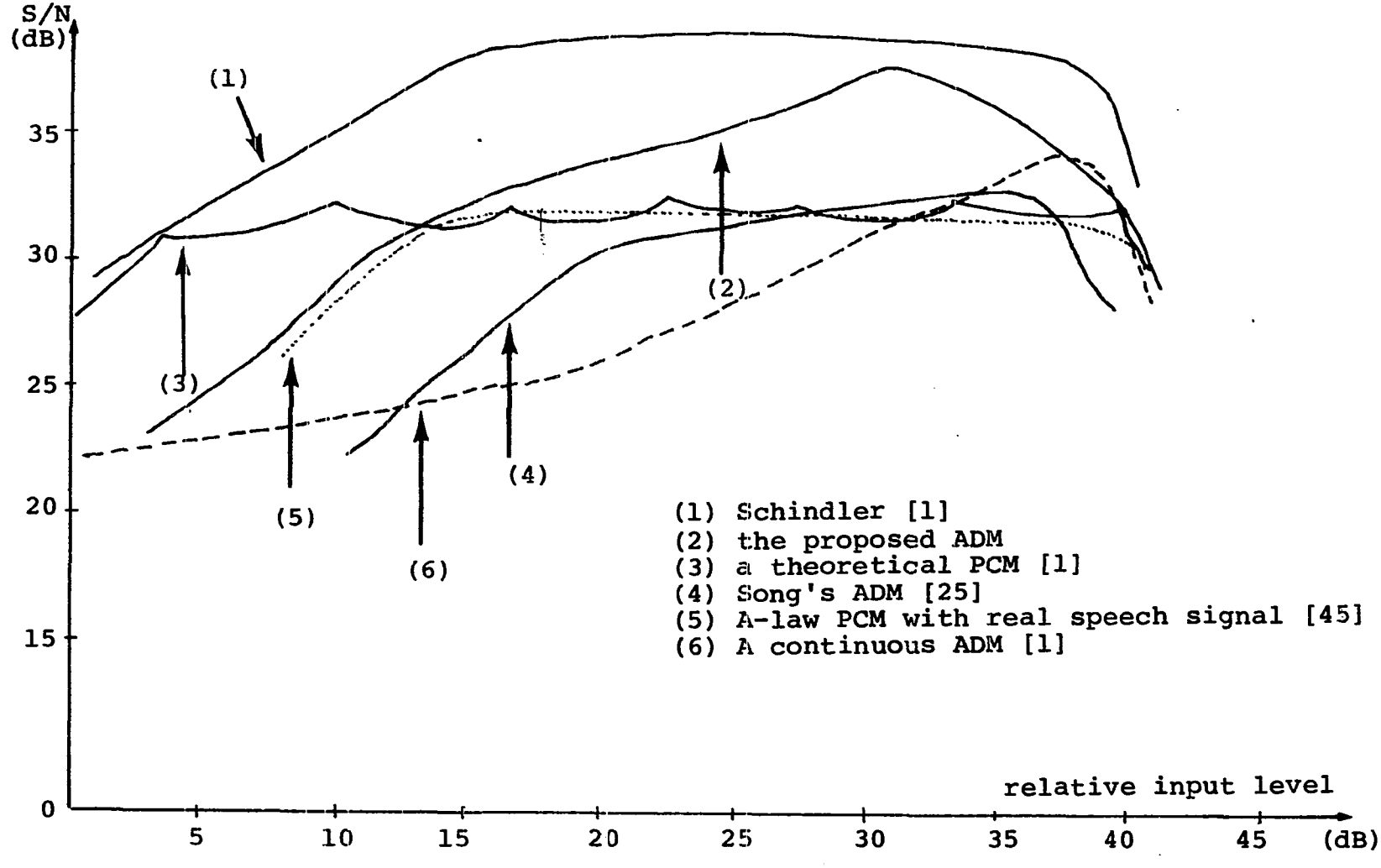

Figure 4.17. A comparison of S/N curves

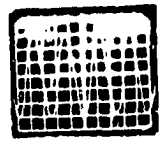

42.8 dB
input
level

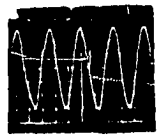

42 dB

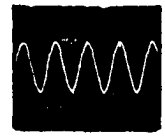

39.4 dB

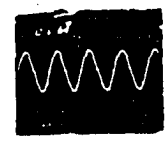

37.5 dB

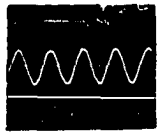

35.8 dB

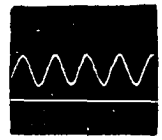

34.5 dB

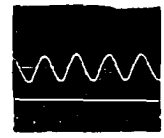

33.3 dB

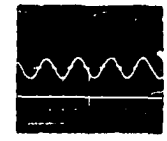

32 dB

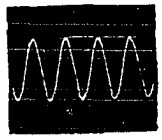

29.8 dB

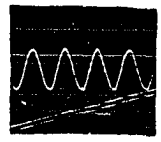

27.3 dB

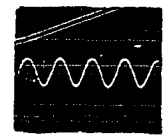

23.8 dB

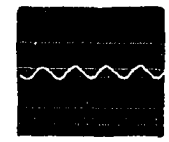

21.7 dB

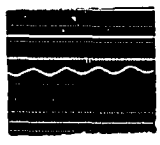

13.7 dB

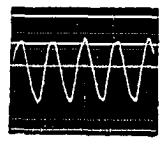

8.7 dB

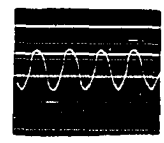

1.3 dB

Figure 4.18. Reproduced sinusoidal waveforms through the band-pass filter for different input levels (20 mV = 0 dB)

Curve (4) also recorded with 800 Hz sinusoidal waveforms is given by Song [27]. Curve (5) measured with simple and real speech signals is given by Schindler [45].

5. SUGGESTED IMPROVEMENTS AND CONCLUSIONS

Once the operating region of the switching amplifier in the system is increased with better analog switches and a lower-drift operational amplifier, the ratio of the largest to the smallest step sizes can be increased. This will, in turn, improve the dynamic range. It is also very likely that the dynamic range can be extended appreciably, especially in the slope overload region, if two or more additional sequences (such as 0000000, 1111111) are used to generate additional (larger) step sizes.

In conclusion, a new hybrid ADM system which adapts its step sizes instantaneously based on n previous bits was proposed, implemented (for n = 4 plus 4 more sequences), and tested with a performance criterion of S/N for 800 Hz sinusoidal waveforms.

After the order of the sequences was derived, partly using Jayant's approach, the step sizes were experimentally determined by choosing the best one out of the three quantizers tried. The low-pass filter inserted in the feedback loop of the system to smooth out abrupt variations in the step sizes was found to improve the system performance significantly. The low-pass filter did cause a slight degradation in the slope overload region, however. Detailed observations were made with pictures of instantaneous

step sizes and reproduced output waveforms. The circuit diagrams of the implemented system were also presented.

The S/N curves measured with sinusoidal input signals were compared with other investigator's results found in the literature. The comparisons show that this system's performance is comparable to other ADM and PCM systems sampled at comparable sampling rates.

6. REFERENCES

1. H. R. Schindler. Delta modulation. IEEE Spectrum 8 (Oct. 1970): 69-78.

2. W. R. Bennett and J. R. Davey. Data Transmission. New York: McGraw-Hill, 1965.

3. P. L. Bargellini. The INTELSAT satellite communications network. News Letter of IEEE Communication Society, Jan. 1975.

4. J. L. Flanagan. Focal points in speech communication research. IEEE Trans. Commun. Technol. COM-19 (1971): 1006-1015.

5. L. R. Rabiner, L. B. Jackson, R. W. Schafer, and C. H. Coker. A hardware realization of a digital format synthesizer. IEEE Trans. Commun. Technol. COM-19 (Dec. 1971): 1020.

6. D. C. Nicholas. Source codes for the output of a delta modulator operating on speech. Ph.D. dissertation, Iowa State University, Ames, Iowa, 1971.

7. M. C. Chow. Variable length redundancy removal coders for differentially coded video telephone signals. IEEE Trans. Commun. Technol. COM-19 (Dec. 1971): 923-926.

8. K. W. Cattermole. Principles of pulse code modulation. New York: American Elsevier Pub. Co., 1969.

9. P. J. Wakeling. Pulse code modulation. London: Mills and Boon, 1972.

10. J. Max. Quantizing for minimum distortion. IRE Trans. Inform. Theory IT-6 (March 1960): 7-12.

11. B. Smith. Instantaneous companding of quantized signals. Bell Syst. Tech. J. 36 (May 1957): 653-709.

12. M. D. Paez and T. H. Glisson. Minimum mean squared-error quantization in speech PCM and DPCM systems. IEEE Trans. Commun. Technol. COM-20 (April 1972): 225-230.

13. J. B. O'Neal, Jr. Predictive quantizing systems (differential puse code modulation) for the transmission of television signals. Bell Syst. Tech. J. 45 (May 1966): 689-721.

14. J. B. O'Neal, Jr. and R. W. Stroh. Differential PCM for speech and data signals. IEEE Trans. Commun. Technol. COM-20 (Oct. 1972): 900-912.

15. R. W. Stroh and M. D. Paez. A comparison of optimum and logarithmatic quantization of speech PCM and DPCM systems. IEEE Trans. Commun. Technol. COM-21 (June 1973): 752-757.

16. P. Cummiskey. Adaptive differential pulse code modulation for speech processing. Ph.D. dissertation, Newark College of Engineering, New Jersey, 1973.

17. B. S. Atal and M. R. Schroeder. Adaptive predictive coding of speech signals. Bell Syst. Tech. J. 49 (Oct. 1970): 1973-1986.

18. J. A. Cadzow and H. R. Martin. Discrete-time and computer control systems. Englewood Cliffs, New Jersey: Prentice-Hall, Inc., 1970.

19. R. W. Stroh. Optimum and adaptive differential PCM. Ph.D. dissertation, Polytechnical Institute, Brooklyn, New York, 1970.

20. P. Cummiskey, N. S. Jayant and J. L. Flanagan. Adaptive quantization in differential PCM coding of speech. Bell Syst. Tech. J. 52 (Sep. 1973): 1105-1118.

21. J. D. Gibson, S. K. Jones and J. L. Melsa. Sequentially adaptive prediction and coding of speech signals. IEEE Trans. Commun. Technol. COM-22 (Nov. 1974): 1789-1796.

22. A. H. Frei, H. R. Schindler, and P. Vettiger. An adaptive dual-made coder/decoder for television signals. IEEE Trans. Commun. Technol. COM-19 (Dec. 1971): 926-944.

23. F. DeJager. Delta modulation, a method of PCM transmission using 1-unit code. Phillips Res. Rept. No. 7 (1952): 442-466.

24. P. T. Nielsen. On the stability of a double integration delta modulator. IEEE Trans. Commun. Technol. COM-19 (June 1971): 364-366.

25. J. B. Abate. Linear and adaptive delta modulation. Proc. IEEE 55 (March 1967): 298-308.

26. J. B. O'Neal. Delta modulation quantizing noise analytical and computer simulation results for Gaussian and television input signals. Bell Syst. Tech. J. 45 (Jan. 1966): 117-141.

27. C. L. Song, J. Gardonick, and D. L. Schilling. A variable-step-size robust delta modulator. IEEE Trans. Commun. Technol. Com-19 (Dec. 1971): 1033-1044.

28. H. Van deWeg. Quantizing noise of a single integration data modulation with n-digit code. Phillips Res. Rept. No. 8 (Oct. 1953): 367-385.

29. D. J. Goodman. Delta modulation granular quantizing noise. Bell Syst. Tech. J. 48 (May/June 1969): 1197-1218.

30. D. L. Schilling and H. Taub. Principles of communication systems. New York: McGraw-Hill, 1971.

31. E. N. Protonotarios. Slope overload noise in differential PCM systems. Bell Syst. Tech. J. 46 (Nov. 1967): 2119-2161.

32. L. J. Greenstein. Slope overload noise in linear delta modulators with Gaussian inputs. Bell Syst. Tech. J. 52 (March 1973): 387-422.

33. D. Slepian. On delta modulation. Bell Syst. Tech. J. 51 (Dec. 1972): 2101-2137.

34. J. B. O'Neal, Jr. Delta modulation of data signals. IEEE Trans. Commun. Technol. COM-22 (March 1974): 334-339.

35. J. A. Greefkes and F. DeJager. Continuous delta modulation. Phillips Res. Rep. 23 (1968): 233-246.

36. S. J. Brolin and J. M. Brown. Companded delta modulator for telephony transmission. IEEE Trans. Commun. Technol. COM-16 (Feb. 1968): 157-162.

37. A Tomozawa and H. Kaneko. Companded delta modulation for telephone transmission. IEEE Trans. Commun. Technol. COM-16 (Feb. 1968): 149-157.

38. T. H. Daugherty. Digitally companded delta modulation for voice transmission. 1970 IEEE Circuit Theory Symposium Digest (1970): 17-18.

39. N. S. Jayant. Adaptive delta modulation with one-bit memory. Bell Syst. Tech. J. 49 (March 1970): 321-342.

40. M. R. Winkler. High information delta modulation. IEEE International Convention Record 8 (1963): 260-265.

41. N. S. Jayant. Digital coding of speech waveforms: PCM, DPCM and DM quantizers. Proc. IEEE 62 (May 1974): 611-632.

42. L. H. Zetterberg and J. Uddenfeldt. Adapted delta modulation with delayed decision. IEEE Trans. Commun. Technol. COM-22 (Sept. 1974): 1195-1198.

43. N. S. Jayant and A. E. Rosenberg. The preference of slope overload to granularity in the delta modulation of speech. Bell Syst. Tech. J. 50 (Dec. 1971): 3117-3125.

44. J. Yan and R. W. Donaldson. Subjective effects of channel transmission errors on PCM and DPCM voice communication systems. IEEE Trans. Commun. Technol. COM-20 (June 1972): 281-290.

45. H. R. Schindler. Linear, nonlinear, and adaptive delta modulation. IEEE Trans. Commun. Technol. COM-22 (Nov. 1974): 1807-1823.

7. ACKNOWLEDGMENTS

The author wishes to express his sincere appreciation to his major professors, Dr. R. G. Brown and Dr. T. M. Scott, for their many valuable suggestions and assistance throughout the course of this study. Their guidance in writing this thesis is deeply appreciated. Also thanks are given to the author's office mate, Mr. R. Rasmussen. Discussions with him on many related subjects were always stimulating and interesting.

Finally, to my parents and uncle to whom the author is indebted for their continuing encouragement and support.

8. APPENDIX A

In this analysis, Max's analysis [10, 15, 16] will be followed. Let us assume an N-level quantizer (Figure A-1).

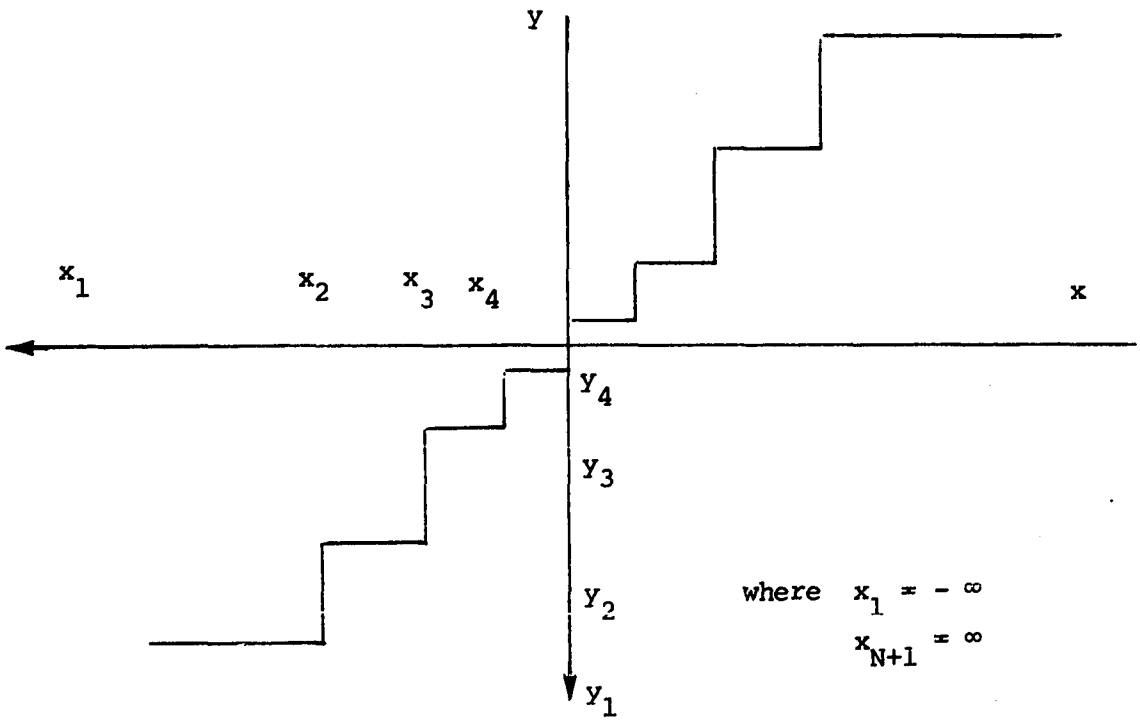

Figure A-1. A quantizer

Then, the output y is given as

$$y = y_i$$

for

$$x_{i-} \leq x < x_{i+1}, \qquad i = 1,2,\ldots,N$$

The error power of the quantizer may be described as follows:

$$E\{(e^2)\} = E\{(y-x)^2\} = \sum_{i=1}^{N} \int_{x_i}^{x_{i+1}} (y_i-x)^2 P(x)\,dx$$

where

$P(x)$ is the probability density function for x.

We want to minimize the mean value of the error.

The derivative of $E(e^2)$ can be written as:

$$\frac{dE(e^2)}{dx_i} = \frac{d}{dx_i} \int_{x_{i-1}}^{x_i} (x-y_{i-1})^2 P(x)\,dx$$

$$+ \frac{d}{dx_i} \int_{x_i}^{x_{i+1}} (x-y_i)^2 P(x)\,dx$$

By the fundamental theorem of calculus, the first condition for the minimum is:

$$\frac{dE(e^2)}{dx_i} = (x_i-y_{i-1})^2 P(x) - (x_i-y_i)^2 P(x) \neq 0$$

Since $P(x) \neq 0$, the above condition reduces to:

$$x_i = \frac{y_i+y_{i-1}}{2} \qquad i = 1,2,\ldots,N \tag{1}$$

The second condition for the minimum is:

$$\frac{dE(e^2)}{dy_i} = \frac{d}{dy_i}\int_{x_i}^{x_{i+1}} (x-y_i)^2 P(x)$$

$$= -2\int_{x_i}^{x_{i+1}} (x-y_i)P(x) = 0$$

Rewriting the equation gives:

$$y_i = \frac{\int_{x_i}^{x_{i+1}} xP(x)dx}{\int_{x_i}^{x_{i+1}} p(x)dx} \qquad i = 1,2,\ldots,N \qquad (2)$$

Since the simultaneous Eqs. (1), (2) cannot be solved analytically for x_i and y_i, a numerical solution is obtained. The approach is outlined as follows:

Choose a value for x_2.

Then by satisfying Eq. (2), find a value for y_i.

Solve Eq. (1) for y_2.

Then the input interval, x_2 to x_3, is calculated from

⋮

This process is repeated until Nth step is reached.

Then check for:

$$\hat{Y}_N = \int_{X_N}^{\infty} xP(x)dx \Big/ \int_{X_N}^{\infty} P(x)dx \qquad (3)$$

$$|\hat{Y}_N - Y_N| < \varepsilon$$

where

ε is the tolerance

If so, solution is good within the specified tolerance. If not, x_2 is decreased when the final value for Eq. (3) is positive, otherwise x_2 is increased.

When P(x) is symmetric with respect to x = 0, $x_1 = \infty$ is changed to $x_1 = 0$ and N is replaced by N = N/2.

9. APPENDIX B

9.1. Mathematical Description

It may be justified that the low-pass filter is omitted in a mathematical analysis for simplicity since the purpose of the low-pass filter is just to smooth out sudden changes in step sizes.

In finding an optimum quantizer in a sense of a least mean-squared error, a mathematical approach is desirable, even though it is unlikely that we can find practical mathematical solutions.

The first step is to define the system in mathematical terms. The objective function P to be minimized is given as:

$$P = \sum_{k=1}^{m} e_k^2 = \sum_{k=1}^{m} (x_k - y_k)^2$$

where

x_k = input known either deterministically or stochastically at a sampling instant

y_k = an estimate of the input

m = is the number of the sampled data

Noting that an integrator can be replaced with a delay memory in an adder of discrete representation, we obtain:

$$y_k = y_{k-1} + F_i(z_{k-1}, z_{k-2}, z_{k-3}, z_{k-4} \cdots z_{k-n}) \times M$$

where the subscripts represent previous states,

F_i is a step size of corresponding sequences z_{k-1},

$z_{k-2}, z_{k-3}, \ldots, z_{k-n}$,

M is a scale factor.

And

$z_{k-1}, z_{k-2}, z_{k-3}, \ldots, z_{k-n}$

are determined by the polarities of e_i's.

That is:

$$z_{k-1} = \text{sgn}(e_{k-1}) = \text{sgn}(x_{k-1}-y_{k-1})$$

$$z_{k-2} = \text{sgn}(e_{k-2}) = \text{sgn}(x_{k-2}-y_{k-2})$$

$$\vdots$$

Therefore,

$$y_k = y_{k-1} + F_i(\text{sgn}(x_{k-1}-y_{k-1}),\ \text{sgn}(x_{k-2}-y_{k-2}),\ \text{sgn}(x_{k-3}-y_{k-3}), \ldots,\ \text{sgn}(x_{k-n}-y_{k-n})) \times M$$

We want to find the optimum $F_i(\ )$'s for each of the sequences to give a least mean-squared error. x_{k-i}'s are known and y_{k-i}'s are previous estimates, so values are known by the recurrent equation. In other words, the above equation is a recurrent equation and may be solved by some recurrent approaches such as dynamic programming.

For an alternative representation, a probabilistic approach may be tried, assuming that the probability distribution of the output sequences for preassigned $F_i(\ )$'s are known or can be measured. If we denote probability density function for the 2^n sequences A_i, $i = 1,\ldots,2^n$

as

$$P(A_i) \quad i = 1,\ldots,2^n$$

where

$$\sum_{i=1}^{2^n} P(A_i) = 1,$$

we can rewrite the expression for y_k as

$$y_k = y_{k-1} + \{\sum_{i=1}^{2^n} F_i(A_i) \times P(A_i)\} \times M$$

The above mathematical description of the system was derived with an object of obtaining optimum quantizers for the system presented here. Several approaches (dynamic programming, and probabilistic methods) were tried in order to find optimum quantizers and were unsuccessful, since the nature of the system is a digital feedback system which is quite complicated.